INTEGRATION OF VCSEL WITH MODULATED RAMAN PUMP FOR DATA AND CLOCK TRANSMISSION IN OPTICAL COMMUNICATION

BY

OSIEMO DOUGLAS MOMANYI

A THESIS SUBMITTED TO THE SCHOOL OF SCIENCE IN PARTIAL FULFILMENT OF THE REQUIREMENTS FOR THE DEGREE OF DOCTOR OF PHILOSOPHY IN PHYSICS, UNIVERSITY OF ELDORET, KENYA

FEBRUARY, 2022

DECLARATION

Declaration by the Candidate

This thesis is my original work and has not been presented for a degree in any other University. No part of this thesis may be reproduced without the prior written permission of the author and/or University of Eldoret.

Osiemo, Douglas Momanyi

Signature…………………...…..   Date…..………………….

SC/PHD/006/16

Declaration by Supervisors

This thesis has been submitted for examination with our approval as University Supervisors.

Dr. David W. Waswa

Department of Physics

University of Eldoret

Signature ……….…………………..... Date…...………………….

Dr. Kennedy Muguro

Department of Physics

University of Eldoret

Signature …………….…………... Date……………………………….

DEDICATION

I dedicate this work to my family and friends for their support.

ABSTRACT

The evolution of ultrafast optical technologies has led to the realization of low cost, low latency and high speed optical networks. Existing telecommunication infrastructure does not provide sufficient capacity to satisfy future demands in terms of extend of coverage, bandwidth and number of served customers. Fibre-optic technology for data transmission is subject to dynamic development fueled by the increasing demand for large bandwidth and reach extension. High capacity VCSELs are the most desired transmitters for data transmission but, they are limited to short distances. Since high powered Raman lasers are compatible with VCSELs, integration of the two unlocks the puzzle of enhanced data and RF clock signal distribution system. First, a 1550 nm VCSEL was directly modulated with 8.5 Gbps data to counter-propagate with modulated backward Raman pump carrying 8.5 Gbps data over a 50.7 km True Wave Reach fibre to realize enhanced full-duplex bidirectional data transmission system. We report error free data transmission with receiver sensitivity of -14.42 dBm, -14.38 dBm and -13.00 dBm for signal analysis with un-modulated backward Raman, modulated backward Raman pump analysis and signal analysis with modulated backward Raman respectively at BER threshold of 10^{-9}. Secondly, unidirectional data transmission system was realized by employing modulated forward Raman pump instead of modulated backward Raman. Modulated Raman pump simultaneously amplifies the VCSEL channel and transmits data over the transmission link, therefore maximizing the network efficiency. Minimum receiver sensitivity of -14.38 dBm was attained for a transmission configuration with un-modulated forward Raman pump. Thirdly, performance of DFB laser on 2 GHz, 4 GHz and 6 GHz RF clock signal distribution was investigated. At 10 kHz offset frequency lowest phase noise of -119.93 dBc/Hz was recorded for 2 GHz signal. Fourthly, we realized a technique of exploiting forward and backward Raman pumping to both disseminate clock tones and amplify data signal simultaneously. 10 Gbps data from directly modulated VCSEL was coupled into a 50.7 km fibre to counter propagate with 4 GHz modulated Raman pump and repeated the same for forward pumping where the data co-propagated with 4 GHz clock. Amplified error-free data transmission with minimum receiver sensitivity of -14.8 dBm for modulated forward Raman and distributed stable clock signal over 50.7 km True Wave Reach fibre was achieved. A maximum phase noise of -100.6 dBc/Hz at 10 kHz offset frequency was experimentally measured for 50.7 km fibre transmission with backward Raman pumping. Finally, long term stability measurement on RF clock signal was analyzed using Allan deviation for DFB laser. Allan deviation of $1.49e^{-12}$ /s and $1.63\ e^{-12}$ /s was obtained for B2B and 24.69 km fibre respectively at 100 s averaging time for 2 GHz clock signal. The results show the suitability of VCSEL light source and Raman amplification for application in integrated optical transmission links. This work offers an integrated VCSEL-based transmission system which satisfy the requirements for the next generation optical fibre networks regarding long reach, enhancement, duplex data/clock dissemination with a single fibre upstream and downstream transmissions.

TABLE OF CONTENTS

LIST OF FIGURES

LIST OF ABBREVIATIONS, ACRONYMS AND SYMBOLS

ASE -Amplified Spontaneous Emission

ATT -Attenuator

B2B -Back to Back

BER -Bit Error Rate

BERT -Bit error Rate Tester

BT -Bias Tee

CD -Chromatic Dispersion

DBR -Diffraction Bragg Reflectors

DCF -Dispersion Compensating Fibre

DFB -Distributed Feedback Laser

DGD -Differential Group Delay

DM -Material Dispersion

DRA -Distributed Raman amplifier

DS -Downstream

DSN -Deep Space Navigation

DSP -Digital Signal Processing

DUT -Device Under Test

DWDM -Dense Wavelength Division Multiplexing

DW -Waveguide Dispersion

EA -Electrical Amplifier

EAM -Electro-Absorption Modulator

EDC -Electronic Dispersion Compensation

EDFA -Erbium Doped Fibre Amplifier

FEC -Forward Error Correction

FTTP -Fibre to the Premises

FWHM - Full Width at Half Maximum

FWM -Four Wave Mixing

GNSS -Global Navigation Satellite Systems

ISI -Inter-Symbol Interference

ITU -International Telecommunication Union

LDC -Laser Diode Controller

LED -Light-Emitting Diode

L -Length

LR -Long Reach

MMF -Multimode Fibre

MZIM -Mach–Zehnder Interferometric Modulator

MZM -Mach-Zehnder Modulator

NASA - National Aeronautics and space Administration

NRZ -Non-Return to Zero

OSNR -Optical Signal to Noise Ratio

PC -Polarization Controller

PD -Photo Diode

PIN -Positive–Intrinsic–Negative Photodiode

PMD -Polarization Mode Dispersion

PON -Passive Optical Network

PRBS -Pseudo Random Bit Sequence Generator

Q -Quality Factor

RA -Raman Amplification

RF -Radio Frequency

R -Reach Fibre

SBS -Stimulated Brillouin Scattering

SMF -Single Mode Fibre

SPM -Self-Phase Modulation

SRS -Stimulated Raman Scattering

SSB -Single Side Band

TIC -Time Interval Counter

US -Uptream

VCSEL - Vertical Cavity Surface Emitting Laser

WAN -Wide Area Network

XPM -cross-phase modulation

P_0 -Output power

P_i -Input power

P_T -Transmitted power

P_0 -Launch power

α -Attenuation coefficient

dB -Decibel

ω -Angular frequency

v_g -Group velocity

τ_g -Group delay

c -Speed of light

β -Propagation constant

n_g -Group refractive index

D -Dispersion parameter

v_d -Drive voltage

q -Electronic charge

V -Volume of the active region

g -Gain

g_0 -Gain coefficient

I_{th} -Threshold current

α -Linewidth enhancement factor

λ -Wavelength

K_p -Polarization constant

P_p -Pump power,

P_s -Signal power

g_R -Raman scattering gain coefficient,

α_s -Signal wave loss

α_p -Pump wave loss

ω_s -Signal angular frequency

ω_p - Pump angular frequency

L_{eff} -Effective length

A_{eff} -Effective area

φ -Fixed phase constant

Δt -Amount of phase deviation,

T -Period

σy -Allan deviation

ACKNOWLEDGEMENTS

CHAPTER ONE

INTRODUCTION

1.1 Background

The constantly growing number of services like high speed Internet, video streaming and conferencing, remote monitoring or ultra-high definition video are the driving force for the next generation communication networks. Limitations of the copper or coax cable bandwidths are already peaking, and in the long term perspective of expected traffic evolution, only optical networks and interconnects can provide enough capacity and flexibility to satisfy the needs. The simultaneous development of semiconductor lasers, optical amplifiers, detectors and high speed electronics, along with the invention of the optical fibre, revolutionized the information technology, allowing to transmit huge amounts of data at unprecedented speed across the world. Optical fibre communication technology has undergone rapid development since the inception of the first-generation optical fibre communication systems in the early 80's, to achieve larger transmission capacity and longer transmission distance. Increase in demand for higher data transmission capacity has been accelerated in the last few years by a rise in internet traffic.

New technologies applications such as Hyper-scale data centers not only require increased data transmission speed but also extended coverage (Isoe, *et. al.*, 2018). Advanced technologies have enabled more data to be transmitted through a single optical fibre over long distances (Prince, *et. al.*, 2011); (Isoe, *et. al.*, 2019). Long-Reach optical network enables broadband access for many customers in the access and metro areas while decreasing operational expenses. High demand for bandwidth

has motivated the invention of new access network architectures to bring high capacity optical fibre closer to end users. Development in passive optical networks (PON) offers potential for unprecedented access bandwidth to consumers. While these PONs offer significant bandwidth improvement, they do not provide the best ultimate solution for service providers seeking to significantly reduce the cost of delivering future broadband services to customers. This led to more far reaching network solutions based on optically amplified long reach PONs (LR-PONs) (Huan, *et. al.,* 2010). The LR-PONs extend the distance between the central office and end users from the traditional range of 20 km to 100 km and beyond, leading to consolidation of metropolitan and access networks (Zhang, *et. al.*, 2014). Optical amplification using erbium doped fibre amplifier (EDFA) in LR-PON is key, but the amplification introduces amplified spontaneous emission (ASE), which has detrimental effect on system performance, for instance, low optical signal to noise ratio (OSNR) (Suzuki, *et. al.*, 2007), that leads to slow speed in adjusting its gain. There is, therefore, need for an improved technology that modifies LR-PONs to transmit amplified data signal and clock signal simultaneously.

Long reach access networks have been proposed as a promising way to reduce the unit cost of bandwidth in fibre-to-the-premises (FTTP) solutions (Koonen, 2005). Systems with symmetric upstream (US) and downstream (DS) data rates of 10 Gbit/s, split factors of 1024 and link lengths up to 135 km have been reported (Davey, 2006). These demonstrations, however, make use of more complicated schemes such as forward error correction (FEC) and electronic dispersion compensation (EDC) and separate fibres and amplifiers for the US and DS channels (Davey, 2006).

Distribution of stable clock signals to remote ends is necessary for applications such as deep-space exploration (Calhoun, *et. al.*, 2007), astronomy and coherent aperture radar (Lau, *et. al.*, 2014). To overcome free space link limitation, transmission of standard frequency over optical fibre has been investigated for years (Foreman, *et. al*, 2007). The technique takes advantage of low attenuation, high reliability and availability of fibres. Reference frequency (RF) frequency has been transferred over 86 km fibre using optical compensator (Lopez, *et. al.*, 2008). Direct optical frequency transfers with better stability and over long distances has been done (Grosche, *et. al.*, 2009). Ultra stable RF transport in NASA antennas have been successfully distributed (Lau, *et. al.*, 2014). Long-distance phase-stabilized 100.02 GHz millimeter (mm) wave distribution over 160 km optical fibre has been demonstrated (Nan, *et. al.*, 2018). Combined optical/RF dissemination system that offers higher stability is being explored. Since optical frequencies have higher order magnitude than RF, they offer corresponding higher stability.

In long distance transmission of signals, it is necessary to compensate for the attenuation losses that occur within the fibre due to various non-linearities and other dominating errors (Agrawal, *et. al.*, 2003). Optical amplifiers are designed to amplify the signal along the fibre. The more the gain of an amplifier, the more the span distance between them, as long as the signal is not distorted due to high optical power (Dahiya, *et. al.*, 2014). The optical amplifiers have been used in many applications ranging from ultra-long undersea links to short links. In data transmission, vertical cavity surface-emitting lasers (VCSELs) are the most desired transmitters for short and intermediate reach systems because of their relatively low fabrication cost and high energy efficiency (Rodes, *et. al.*, 2010; Olmos, *et. al.*, 2012). In addition,

VCSELs high bandwidth, wavelength tunability and direct modulation capability (Rodes, 2012); (Tatum, 2015). But VCSEL technology is limited to low optical power and frequency chirping due to fibre dispersion within fibre transmission length thereby limiting attainable reach (Isoe, *et. al.*, 2019).

To overcome the problem of lower power signal optical amplification stimulated Raman scattering (SRS) is employed. The SRS is used regularly in modern optical communications systems, especially the distributed amplification which offers significant advantages as compared to lumped amplifiers such as EDFA. EDFA suffers from amplified spontaneous emission (ASE), which increases noise figure (Laming, *et. al.*, 1988). There is a constant progress and growth on long wavelength data transmission using VCSELs as light sources. VCSEL is a special laser diode that has revolutionized fibre optic communications by improving efficiency and increasing data speed. Use of vertical cavity surface-emitting lasers (VCSELs) and Raman amplification to transmit high speed data signals over optical fibre has been experimentally demonstrated (Kiboi, *et. al.*, 2018). Direct modulation of 1550 nm VCSELs at 40 Gb/s has been demonstrated (Hofmann, *et. al.*, 2011). Advancement in performance and reliability of long wavelength (1550 nm VCSEL) opens the possibility of using them in optical access networks. But these VCSELs require tight power budget due to poor tolerance to fibre chromatic dispersion. However, this dispersion can be compensated by using dispersion compensating fibres (DCFs) which increases dispersion limited transmission distance at 1550 nm in VCSEL based systems (Hofmann, *et. al.*, 2009); Prince, *et. al.*, 2010). These approaches are not practical enough to be used for cost effective optical access networks since they require costly and bulky optical components, e.g. additional optical amplifiers to the

system. Free-running 1550 nm VCSEL directly modulated at 10.7 Gb/s reported successful error-free transmission through 40 km of standard single-mode optical fibre without the use of dispersion-mitigation (Prince, *et. al.*, 2011). Long reach extension has been demonstrated using high-speed oxide-confined 1060 nm single and multimode VCSELs for extended reach VCSEL-multimode fibre (MMF) optical interconnects (Larsson, *et. al.*, 2018). Large bandwidths and small delays are the driving forces in the continued development of technology and thus need for a technology that meets these standards. Raman amplification has been used to extend reach by adopting VCSEL four level pulse amplitude modulation and dense wavelength division multiplexing (DWDM) (Isoe, *et. al.*, 2018). Because data networks are developing more and more into critical infrastructures, enhanced unidirectional and bidirectional duplex data transmission for ultra-long haul networks and wide area networks (WAN) is also a very relevant topic. Monolithic integration, and operation of 850-nm wavelength based vertical cavity surface-emitting lasers (VCSELs) and PIN (p-doped–intrinsic–n-doped) photo-detectors has been reported (Alexander, *et. al.*, 2013). From this work a real-time technique for transmitting accurate data and a stable clock signal for long-reach optical networks employing forward Raman pumping was presented. Recently, for the first time, integrated cross-modulated forward Raman pump with power efficient VCSELs for simultaneous data amplification and transmission was reported (Isoe, *et. al.*, 2019). The main motivation of integrating Raman amplification with VCSELs to simultaneously transmit enhanced data and clock signals is the compatibility and their numerous advantages such as broad bandwidth, high saturation input power and low noise figures.

1.2 Statement of the problem

Distribution of information in a fast changing world are hindered by high-cost and low speed integrated systems. Data and RF clock can be transmitted in optical fibre, but signal losses frustrates the desirable integrity and limits transmission distance. Advancement in performance and reliability of long wavelength VCSEL opens the possibility of using them in next generation networks. But these VCSELs are limited to low optical power and frequency chirping due to dispersion within the fibre. Existing approaches are not practical enough to be used since they require costly and bulky optical components, e.g. additional optical amplifiers to the system. Because data networks are developing more and more into critical infrastructures, enhanced full duplex data/clock transmission for ultra-long haul networks is long overdue. There is also a challenge in the distribution of coherent frequency sources over long distance with minimal perturbation. Optical fibre has been utilized to disseminate stable radio frequency signal and data over long distance independently. Transfer of stable reference frequency (RF) and data over long distance has only been achieved using different links thus increasing the cost. The use of Raman amplification technology for long haul transmission has only been utilized to transmit amplified data so far. There is, therefore the need to utilize Raman pump to both enhance VCSEL and transmit data/clock signal.

1.3 Objectives

General objective

To demonstrate transmission of data and clock using a single link over extended reach with Raman Pump reuse.

Specific objectives

The specific objectives of the study were:

i.   To evaluate signal data performance (VCSEL) under forward and backward Raman pumping

ii.   To integrate modulated Raman pump in VCSEL technology for simultaneous data and timing signals distribution

iii. To characterize the RF clock signal stability on the modulated pump wavelength performance

iv.   To characterize stability of distributed RF clock signal using DFB laser

1.4 Justification of the study

Data transmission in optical fibre require enhancement to achieve the last mile goals. This can be achieved by combining Raman amplification and low cost VCSELs in data and clock distribution. The study is of great significant in enhancing long wavelength VCSELs transmission of error-free data and utilize modulated Raman to disseminate stable clock signals for distances above 50 km. Therefore, Raman pumps which are compatible with VCSELs can be integrated to extend reach for VCSELs and at the same time reuse Raman laser to transmit data and clock signal. The advantage of low phase noise and the ability to amplify the signal and transmit clock makes Raman pump suitable for data signal enhancement and clock distribution. Backward Raman pumping provides an important feature for duplex bidirectional transmission while forward pumping provides the unidirectional feature. Combined data and clock dissemination over a single fibre reduces complexity and cost hence meeting next generation infrastructure requirements. Configuration flexibility, compatibility with widely accepted standards and transparency for transmitted data

continues to make this technology attractive for commercial optical network operators. This work offers to enable techniques for improving network capacity, efficiency, low cost and reach optimization for next-generation optical interconnects.

CHAPTER TWO

LITERATURE REVIEW

2.1. Introduction

This chapter gives a brief review for optical fibre communication fundamentals, optical transmitters, Raman amplification in optical communication systems, RF clock dissemination, system performance and Modulated Raman pump in VCSEL technology for simultaneous data and clock distribution.

2.2 Optical Fibre Communication Fundamentals

2.2.1 Impairments in Optical Fibres

An optical fibre link is used to transport the data from a transmitter to a receiver without distorting and corrupting the data. Almost all light wave telecommunication system used optical fibre as a transmission medium because of their high capacity, low optical attenuation properties and high resistance to electromagnetic interference. As the telecommunication systems evolved to higher bit rates and transmission distances increase, linear and non-linear effect experienced by optical signals propagating along the fibre becomes the limiting factors (Agrawal, 2006). When low power is launched into the fibre, optical communication systems experience linear effects which include; signal attenuation and dispersion. Increasing power input leads to nonlinear effects in the fibre. These effects in optical fibre arise from the intensity dependence of the refractive index and they include stimulated Brillouin scattering (SBS), stimulated Raman scattering(SRS), four-wave mixing (FWM), cross-phase modulation (XPM) and self-phase modulation (SPM). (Agrawal, 2007).

2.2.2. Attenuation

The propagation of a pulse in the core of the optical fibre causes power attenuation resulting to a reduction in output optical power. Attenuation of the light signal as it travels along the fibre is a key consideration in the design of an optical communication system and is one of the limiting factors that degrades the quality of the optical signal during transmission. In a standard SMF, the total transmitted power P_T over a distance L is given as (Agrawal, 2001):

$$P_T = P_0 e^{(-\alpha L)} \tag{2.1}$$

where P_0 is the launch power and α is the attenuation constant of the fibre. The α is given by

$$\alpha \left(\frac{dB}{km} \right) = -\frac{10}{L} Log_{10} \left(\frac{P_T}{P_0} \right) \tag{2.2}$$

and is expressed in units of dB/km (Agrawal, 2001). Figure 2.1 shows the variation of α with the wavelength of light signal.
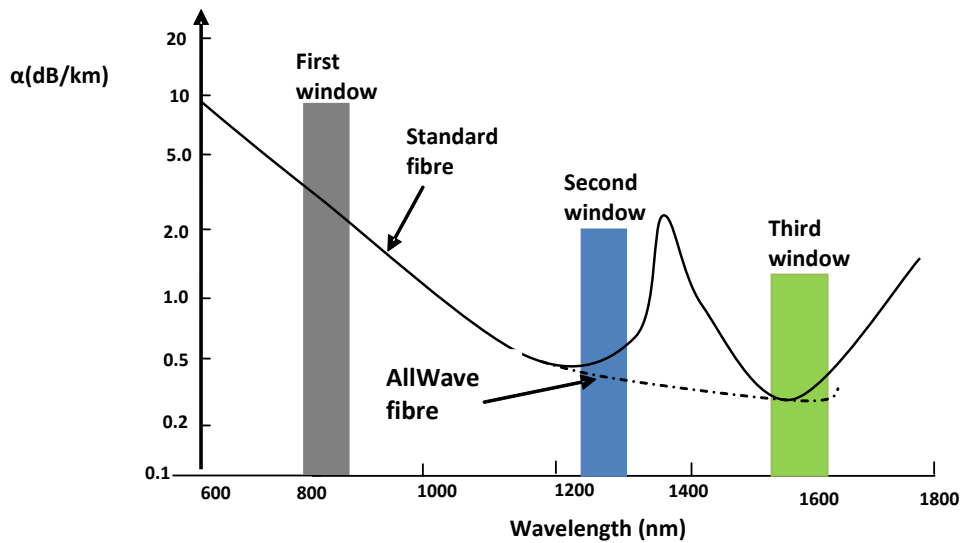
Figure 2.1: Optical fibre attenuation as a function of wavelength

Optical attenuation stems from fibre related intrinsic and extrinsic effects. Fibre losses are considerably higher for shorter wavelengths and exceed 5 dB/km in the visible region making them unsuitable for long distance transmission. Silica fibre has typical attenuation of about 0.2 dB/km at the wavelength of 1550 nm (Agrawal, 2002). Intrinsic effects include mechanisms such as material absorption and Raleigh scattering of light within the fibre core region. On the other hand, extrinsic loss mechanism includes bending losses, core/cladding losses, splice and connector losses.

2.2.3. Chromatic Dispersion (CD)

A modulated optical signal propagating along a fibre consists of an infinite number of spectral components with an associated frequency, ω. The individual spectral components propagate independently to each other with distinct group velocities, v_g, therefore, resulting in the propagation group delays, τ_g. The group velocity is expressed as:

$$v_g = \left(\frac{d\beta}{d\omega} \right)^{-1} = \frac{c}{n_g} \qquad (2.3)$$

where β refers to the propagation constant and n_g is the group refractive index. Equation (2.3) illustrates the frequency and refractive index dependence on group velocity. Consequently, the individual spectral components propagate at different group velocities, thereby causing the pulse to spread and broaden over time. This phenomenon is referred to as chromatic dispersion. The overall broadening experienced by the propagating pulse due to the chromatic dispersion (CD) along the optical fibre is defined as (Agrawal, 2002):

$$\Delta\tau = L \frac{d^2\beta}{d\omega^2} \Delta\omega \qquad (2.4)$$

where L is the fibre length and $d^2\beta/d\omega^2$ is a second-order derivative of propagation

constant and $\Delta\omega$ is spectral range given by:

$$\Delta\omega = \left(-\frac{2\pi c}{\lambda^2}\right)\Delta\lambda \qquad (2.5)$$

The CD coefficient or dispersion parameter is expressed as,

$$D = \frac{1}{L}\frac{\Delta\tau}{\Delta\lambda} = \frac{d}{d\lambda}\left(\frac{1}{v_g}\right) = -\frac{2\pi c}{\lambda^2}\beta_2 \qquad (2.6)$$

The units of D is ps/(nm.km). Chromatic dispersion can be written as CD=DM+DW,

where DM and DW refer to material and waveguide dispersion respectively. Material

dispersion arises because of the change in refractive index of silica with optical

wavelength or frequency. Waveguide dispersion occurs due to the wavelength

dependence of core diameter as well as the refractive index difference (Agrawal,

2002).

2.2.4 Polarization Mode Dispersion (PMD)

Polarization-mode dispersion in optical fibres arises due to birefringence where

propagation constant β changes with respect to two polarization axes in x (fast) and y

(slow) directions during propagation. Birefringence and modal dispersion are the two

effects responsible for PMD within the fibre. Apart from CD, PMD is another source

of pulse broadening within the optical fibre, arising from the difference in the group

velocities of the two orthogonal polarization Eigen modes (Keiser, 2011). Time delay

ΔT between the two polarization components due to random changes in group

velocities broadens the optical pulse (Agrawal, 2007) and if ΔT is large enough so

that stretched pulse overlaps with the neighbouring time slot it will cause inter-symbol interference.

$$\Delta T = \left| \frac{L}{v_{gx}} - \frac{L}{v_{gy}} \right| = L\left| \beta_{1x} - \beta_{1y} \right| = L(\Delta\beta_1) \qquad (2.7)$$

where $\Delta\beta_1$ is related to group velocity mismatch. The degree of modal birefringence was quantified by Kaminov, (1981) as:

$$\beta_m = \frac{\left| \beta_x - \beta_y \right|}{k_0} = \left| n_x - n_y \right| \qquad (2.8)$$

where k_0 is the core radius. The length of the full rotation of polarization state is called beat length L_B and can be expressed as (Kaminov, 1981)

$$L_B = \frac{2\pi}{\left| \beta_x - \beta_y \right|} = \frac{\lambda}{B_m} \qquad (2.9)$$

Refractive index and birefringence varies along the span length therefore PMD should be estimated by averaged time delay:

$$\sigma_T^2 = \left\langle (\Delta T)^2 \right\rangle = 2(\Delta\beta_1 l_c)^2 [\exp(-L/l_c) + -L/L_C - 1] \qquad (2.10)$$

where L_C is the length over which two polarizations are correlated (correlation length). With the assumption that correlation length is much smaller than the span length, equation (2.10) can be simplified to

$$\sigma_T \approx \Delta\beta_1 \sqrt{2L_C L} \equiv D_p \sqrt{L} \qquad (2.11)$$

where D_p is the PMD parameter used in fibre characterization. PMD effect will have a relatively small impact on pulse broadening comparing with group velocity dispersion

(GVD). However, in high data rate communication systems operating near zero-dispersion wavelength PMD will degrade the transmission quality (Agrawal, 2005)

2.3 Optical Transmitters

The crucial role of optical transmitter is to convert an electrical information input signal into its corresponding optical domain, which would then be launched into an optical communication channel, the fibre. Transmitters are basically semiconductor devices, such as light-emitting diodes (LEDs) and laser diodes.

2.3.1 Distributed-Feedback (DFB) Semiconductor Laser and Raman pump

In a DFB laser, as the name implies, the optical energy feedback mechanism is not localized at the facets but is distributed throughout the cavity length. Figure 2.2 shows the structure for distributed feedback laser (DFB).
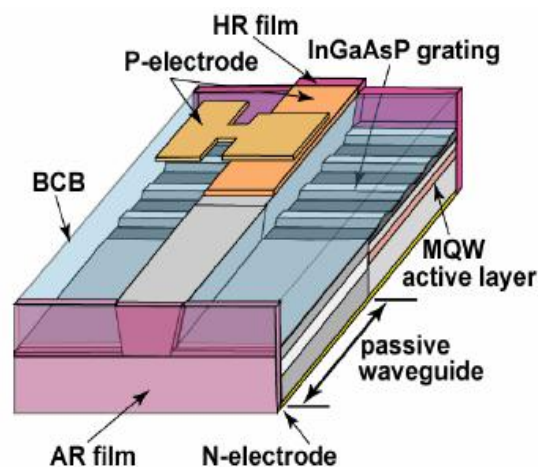
Figure 2.2: Structure of DFB laser

The DFB lasers employ Bragg diffraction gratings in the active gain region of the semiconductor to form a waveguide (Li, *et. al.*, 2013). Light travelling in the active layer move in all directions, and so will eventually strike the upper surface of the active layer. In this way, the corrugations act as a grating, reflecting only a specific

wavelength back into the cavity but allowing others to pass through. The desired wavelength is fed back into the cavity, and this takes place over the whole length of the laser, therefore achieving the distributed feedback. In DFB lasers, one axial resonator mode prevails over the other modes. This yields a relatively narrow single mode emission peak at the desired wavelength. Commercial DFB lasers have a typical linewidth of 1-10 MHz. Narrow-linewidth laser sources are useful for many diverse applications, including coherent communication, stable frequency standards, nonlinear optics, and precision sensing (Tadokoro, *et. al.*, 2011; Steger, 2014; Dhoore *et. al.*, 2019). The oscillation wavelength of the DFB laser is determined mainly by the equivalent refractive index of the grating region and the grating pitch (Katsuyama, 2009). The grating applied to DFB laser is formed by electron beam lithography or laser interference lithography, etching and subsequent planar buried growth (Dhoore *et. al.*, 2019). Numerous advantages of a DFB laser diode over other laser types such as their stable single-mode spectrum, high output power, integration compatibility and low noise operation make it an attractive source for many applications.

2.3.2 Continuous wave (CW) Raman laser

Top view structure for CW Raman laser is shown in Figure 2.3.
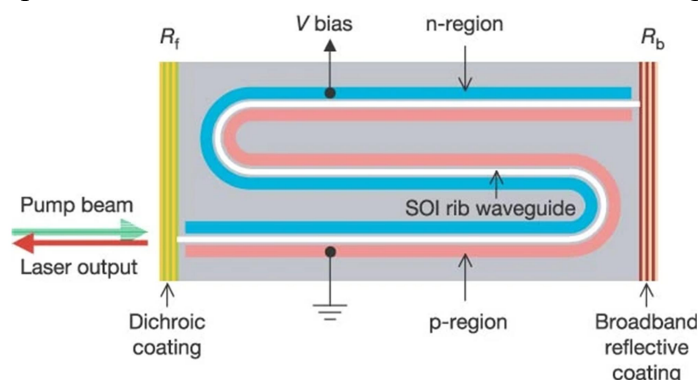
Figure 2.3: Schematic diagram showing the structure of the CW Raman pump.

The light is confined in the S shaped waveguide formed by using Silicon-On-Insulator (SOI) structure. The intrinsic (i) Si layer in the p-i-n structure guides the light. External bias is applied to the p and n layers surrounding the intrinsic(i) layer on its two sides. Stimulated Raman scattering (SRS) and amplification take place in the S-shaped region labeled as SOI rib waveguide. The actual material (SOI) is intrinsic silicon surrounded by two p and n-type regions of Si on its two sides and a layer of silicon oxide (insulator) beneath it (Rong, *et. al.*, 2005). There are three essential components in a laser:

i. An active medium in which amplification of light wave takes place due to stimulated emission.

ii. A mechanism to provide positive feedback to amplified radiation to enable emission of self-sustained oscillation

iii. A pump source which lifts the electrons from the ground state to an excited state to create population inversion between the excited and ground states.

The active Si region in which SRS occurs, is surrounded on its two sides by lower refractive index p- and n-type silicon (Basu, 2007). Light is then confined in the higher index Si region, much in the same manner as light is guided in the core of an optical fibre. The two plane parallel mirrors, R_f and R_b provide the feedback. The emission of Stokes radiation is quite feeble for low pump power. However, as the pump power exceeds a threshold, stimulated process dominates and as a result, the Stokes intensity increases rapidly with increase in pump power. This pump laser is still an optically pumped source. However, in all applications related to electronics, computer and communication, it is necessary that the control should be by an external

electrical bias (Basu, 2007). The fundamental linewidth limit of most lasers originates from the spontaneous emission coupled to the lasing mode (Honjo, *et. al.*, 2011).

2.3.3 Vertical Cavity Surface Emitting Lasers (VCSELs)

One of the key advances in optical communication technology in recent years is the development of vertical-cavity surface-emitting laser (VCSEL). The concept of the VCSEL was first proposed by Iga in 1977 (Iga, 1977; Iga, 2000), and the first working devices were subsequently reported later by the same group (Soda, *et. al.*, 1979). This laser has entirely replaced edge-emitting laser diodes for use in multimode fibre based Giga bit per second (Gbps) speed optical data transmission in premise networks for the interconnection of various kinds of computer clusters. Early VCSELs were based on technologically challenging InGaAsP material system (Hahn, *et. al.*, 1999). A breakthrough occurred in the late 1980s with the demonstration of the first continuous-wave operating GaAs-based VCSEL using metal and dielectric mirrors (Levi, 2000; Trezza, *et. al.*, 2003). Full monolithic InGaAs-GaAs lasers incorporating epitaxial distributed Bragg reflectors with emission wavelengths of about 960 nm and pulsed threshold currents of 1.3 mA were demonstrated in 1989 (Windover, 2005). VCSELs were first commercially availed by Honeywell in 1996. As a result of standardization, these first generation lasers were made from GaAs-AlGaAs mixed compound semiconductors for emission close to 850 nm and relied on proton implantation (Dolfi, 2003; Drögemüller, *et. al.*, 2000) for current confinement. The success of the VCSEL arises from a combination of unique properties. With the main emphasis on optical data transmission, VCSEL has high performance and low cost advantages (Company, 2013)**.** Other important merits include:

1. Low threshold current and low power consumption with a small active region.

2. Feasibility of tightly packed two-dimensional integration.

3. Single longitudinal mode operation due to large mode spacing.

4. High coupling efficiency into a fibre due to low divergence circular beam profile that matches the fibre mode.

5. Wafer-level testing before packaging. Complete testing and device selection on the wafer level, yielding enormous cost reduction

6. High speed modulation capability due to the large relaxation oscillation frequency.

7. Batch fabrication processing used in silicon technology.

8. Testability: VCSELs can be tested and burned in while still in wafer form. This increases manufacturing yield and lowers the cost of production.

9. Integration with integrated optics and electronic circuits.

2.4 Raman Amplification in Optical Communication Systems

The scattering of light waves by impurities can occur due to the absorption through vibration of the electrons and dislocation of molecules in silica-based materials. Scattering processes in which the frequency of the light wave carrier is shifted to another frequency region are commonly known as inelastic scattering. The ability of light to scatter inelastically on a molecular structure and exchange energy with the material was discovered by an Indian Physicist C. V. Raman in 1928 (Raman, 1928). Raman amplification attracted much interest in 1962 when the phenomenon of stimulated Raman scattering was first discovered (Woodbury and Nag, 1962).

2.4.1 Stimulated Raman Scattering (SRS)

Raman scattering is due to inelastic nonlinear behavior of a dielectric medium when subjected to a high intensity optical beam (Raman, 1928; Clifford *and* Agrawal, 2005). There are two levels of scattering namely; Stokes Raman scattering occurring when the final energy level of the molecule is higher than the initial level, anti-Stokes Raman scattering occurring when the final energy level is lower than the starting level. The Stokes scattering is much more common than anti-Stokes scattering because at any given time an electron in the most common temperature range is most likely to be in its lowest energy state, following the Boltzmann distribution (Parakhan, 2009).

2.4.2 Raman Amplification Processes

The SRS occurs in silica-based fibre when a pump laser source is launched into the guided medium. The scattering light from the molecules and dopants in the core region shifts to a higher energy level and then jumps down to a lower energy level, thereby amplifying photons in this level. The virtual state as shown in Figure 2.4 is due to the fact that Raman scattering is non resonant and is therefore a very fast process (Stolen *et. al.*, 1989).
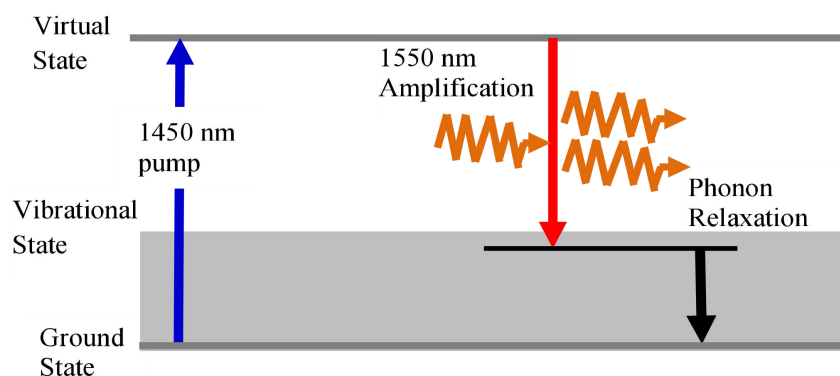
Figure 2.4: Description of the SRS process quantum mechanically

The phenomenon of the SRS process is described quantum-mechanically as the scattering of a photon by one of the molecules to a lower-frequency photon, while the molecule makes a transition to a higher-energy vibrational state (Agrawal, 2007). The pump photon is converted to a second signal photon that is a replica of the first and the remaining energy is converted into an optical phonon. The continuum nature of molecular vibration state is due to the amorphous nature of silica, i.e. silica has inconsistent physical and chemical properties. This distributes the energy of a medium to different wavelengths (Clifford and Agrawal, 2005).

At high power levels, the nonlinear phenomenon of SRS leads to remarkable signal amplification in the fibre transmission span. The intensity of the scattered light grows exponentially as the incident power exceeds a given threshold value. The threshold power is the minimum power level at which the Raman process becomes stimulated and transfers most of the pump power to the Stokes wave (Clifford and Agrawal, 2005). It exists when the transmitted power of a channel exceeds the threshold power given by equation (2.15) for a single light wave channel (Pelouch, 2016).

$$P_{th} = \frac{16.A_{eff}}{K_p.L_{eff}.g_r}$$ (2.12)

where K_p is the polarization constant and assumes a value of 2 for a completely unscrambled signal. The scattering occurs when the polarization of the molecule changes with vibrational motion.

As anti-stokes scattering is initiated in the excited vibrational level its transition rate is also proportional to this distribution. In SRS, because of the relative intensities, the Stokes shift is an essential element in the design of Raman amplifiers (Singh, *et. al.*, 2007). Raman gain bandwidth is defined as the Full-Width at Half Maximum

(FWHM) of the dominant peak in the gain spectrum. The overall optical gain can be expressed in terms of the pump intensity I_p:

$$g(v) = g_R(v)I_p = g_{R0}(v).\left(P_p / A_{eff}\right) \qquad (2.13)$$

Equation (2.16) shows that the gain is dependent upon the frequency and the pump power.

2.4.3 Raman Gain Curve

The power evolution of the pump (Pp) and signal (Ps) along the direction of propagation z, can be represented by a set of two coupled equations:

$$\frac{dP_s}{dz} = g_R P_P P_s - \alpha_s P_s \qquad (2.14a)$$

$$\xi\frac{dP_p}{dz} = \frac{\omega_p}{\omega_s} g_R P_P P_s - \alpha_p P_p \qquad (2.14b)$$

where g_R is the Raman gain coefficient, α_s and α_p are the attenuation coefficients of signal and pump waves respectively, ω_s and ω_p are signal and pump angular frequencies respectively. The parameter ξ takes values of + or - depending on the pumping configuration. The minus sign is used in the backward pumping case. The frequency ratio $\frac{\omega_p}{\omega_s}$ appears in equation (2.17b) because the pump and signal photons have different energies. The spectrum of the Raman gain depends on the decay lifetime of the excited electronic vibration state.

Figure 2.5 shows that Raman gain in silica fibres extends over a large frequency shift

(up to 40 THz) with a broad peak located near 13 THz.
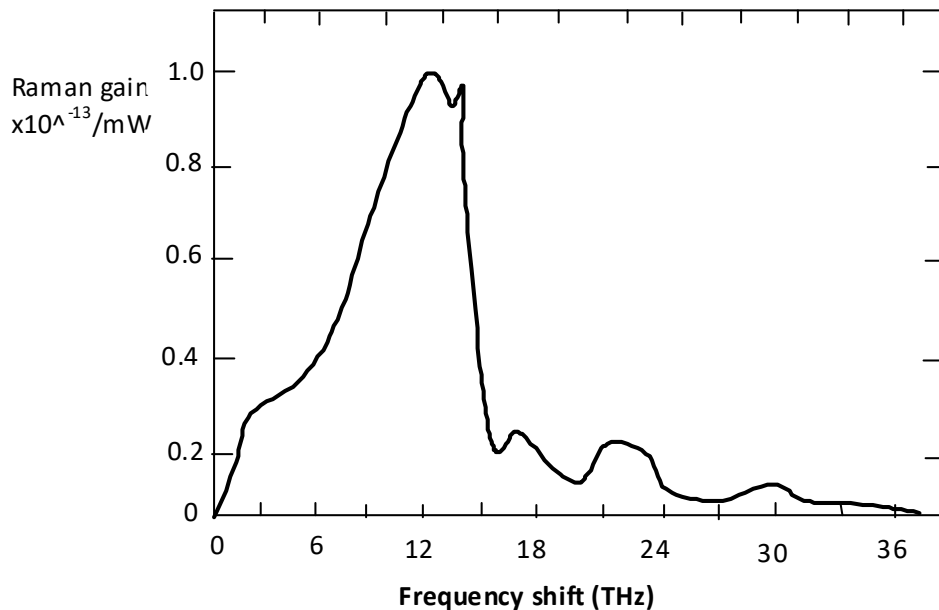
Figure 2.5: The gain curve for SRS

This behavior is due to the non-crystalline nature of silica fibre. Therefore, maximum

gain occurs when the pump-signal detuning is about 100 nm.

2.4.4 Pumping Configuration

Pumping in different directions changes the signal power evolution along the length

of the fibre. Three pumping schemes are employed namely; forward (co-pumping),

backward (counter pumping) and bi-directional (achieved when both forward pump

and backward pump are on) as shown in Figure 2.6 (Xueming, 2004; Isoe, *et. al.*,

2013). In the forward pumping, there is a large gain in power at the beginning of the

fibre length. This can result into fibre non-linearities (or non linear effects) due to the

fact that the refractive index of the core and cladding is optical power dependent. In

backward pumping large gain occurs towards the end of the fibre after a substantial

signal power loss. This power loss increases the possibility of noises altering the

quality of the signal. The bidirectional scheme shows a balanced result in terms of noises and non-linearities. The power along the length of the fibre is gradually reduced by the losses. These result in microscopic fluctuations in the density of the core. Doping the fibre with dopants such as germanium further increases these losses. It is also a limiting factor in transmission distance lengths as optical receivers require a minimum amount of power to recover the signal.

A schematic of Raman amplifier as optical communication system is shown in Figure 2.9. The signal from the optical transmitter propagates through the optical fibre and is detected at the receiver side using a photodiode.
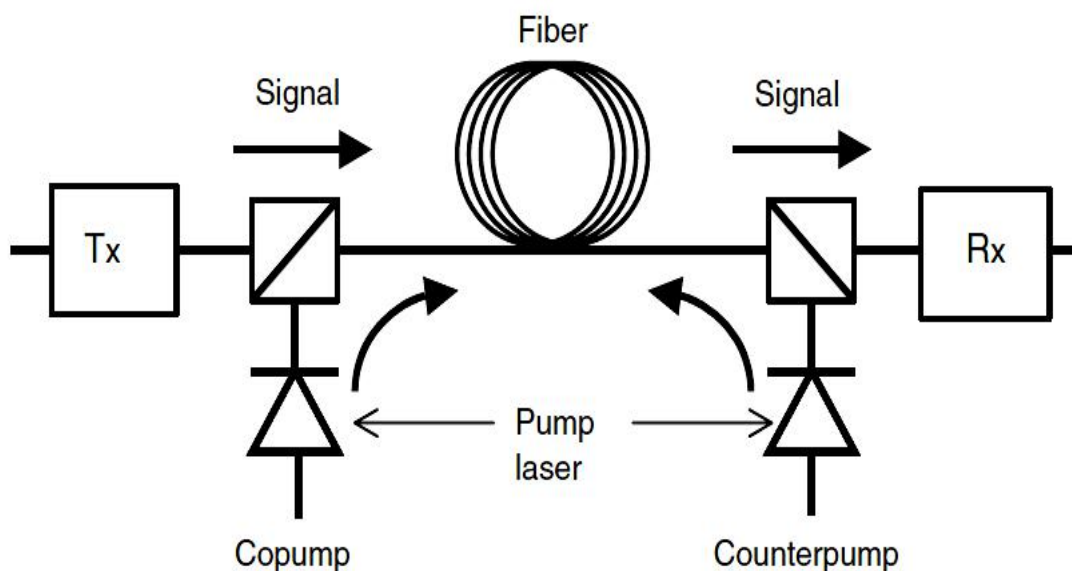
Figure 2.6: Bidirectional pumping configuration.

For a distributed Raman amplifier (DRA), power is provided by Raman pump whose wavelength is shorter than the signal wavelength. The signal is amplified by an amount that corresponds to an optical frequency difference of about 13.2 THz (Islam, 2004). The signal then experiences gain due to SRS. If the pump depletion can be neglected, that is in the small-signal amplification regime, the pump-power for forward pumping decreases according to the relation:

$$P_p(z) = P_0 \exp(-\alpha_p z) \qquad (2.15)$$

where P_0 is the pump-power at the input. The effective length L_{eff}, is the length over which the nonlinearities still hold or SRS occurs and is defined as:

$$L_{eff} = \frac{1 - \exp(-\alpha_p L)}{\alpha_p} \qquad (2.16)$$

As losses also exist at the pump wavelength, it is less than the actual length and can be approximated by $L_{eff} \approx 1/\alpha_P$ if $\alpha_P L \gg 1$. Hence, the amplification gain defined as the ratio of the power of the amplified signal to that of the signal without Raman amplification and is given by:

$$G_A = \frac{P_S(L)}{P_S(0)\exp(-\alpha_S L)} = \exp(g_0 L) \qquad (2.17)$$

Equation (2.17) is referred to as the on-off Raman gain and it is the difference in power of the signal with Raman amplification and signal power without Raman amplification. The small-signal gain, g_0 is defined as:

$$g_0 = \frac{g_R P_0}{A_{eff} \alpha_p L} \qquad (2.18)$$

where A_{eff} effective area.

Stimulated Raman scattering is applied in several disciplines. In biomedicine, SRS can be used in coherent Raman microscopy which allows highly sensitive optical imaging at video rate (Saar, *et. al.*, 2010). Photonics crystal fibres make use of highly nonlinear holey fibre to generate Raman amplification and ultrafast signal modulation (Yusoff, *et. al.*, 2002). Silicon waveguide technology uses SRS for on-chip

amplification and coherent light generation in silicon integrated optics (Claps, *et. al.*, 2004). Other application are optical sensing where backscattered light may be used to measure temperature (Dakin and Pratt ,1985), fibre-based Raman lasers (Yan, *et. al.*, 2009) and Raman amplifiers (Chinlon, *et. al.*, 1976; Islam, 2003; Clifford and Agrawal, 2005) which gained the main interest in high capacity optical communication systems where low noise amplification is crucial. Raman amplification is a key developmental technology to improve performance of the optical fibre network. This technology provides technical advancements to optical long haul transmission infrastructure. However, Raman amplification requires a high pump power to provide a reasonable gain and suffers from signal cross talk when the channel power is above threshold power resulting in overall signal degradation.

2.5 RF Clock Dissemination

2.5.1. Timing Signals, Accuracy and Stability

A clock is comprised of a stable oscillator and a device to count the oscillator's cycles. Naturally, it can be used to generate a timing or a frequency signal. Time transfer methods are used to transfer time and/or frequency information from a reference clock at one location to a remote location. An ideal sine wave oscillator produces a voltage signal that changes with time and is given by:

$$V(t) = A\cos[\omega_0 t + \varphi] \tag{2.19}$$

where A is the amplitude, ω_0 the angular velocity and φ represent a fixed phase constant. However, in a real oscillator, the actual clock signal fluctuates in phase and amplitude, where the output is described as

$$V(t) = A[1 + \alpha(t)]\cos[\omega_0 t + \varphi(t)] \tag{2.20}$$

where $\alpha(t)$ and $\varphi(t)$ represents the random amplitude and phase fluctuations (Stefano, 1997). The performance of an oscillator is given by its accuracy and stability characteristics.

Accuracy is the degree of conformity of a measured or calculated value to its true value, that is accuracy is related to the offset from the ideal value. For example, frequency offset is the difference between a measured frequency and an ideal frequency with zero uncertainty. The frequency offset is expressed by:

$$f_{offset} = \frac{f_{measured} - f_{nominal}}{f_{nominal}} \tag{2.21}$$

where $f_{measured}$ is the frequency of the counter and $f_{nominal}$ is the frequency indicated on the oscillators nameplate. A simple phase comparison can be made with an oscilloscope. If the two input signals have the same frequency, the time interval will not change. If the two signals have different frequencies the time interval will change. The resolution of a time interval counter (TIC) determines the smallest frequency change that it can detect without averaging. The current limit for TIC resolution is about 20 ps, which means that a frequency change of 2×10^{-11} can be detected in 1 second. Averaging over longer intervals can improve the resolution to < 1ps in some units.

Stability indicates how well an oscillator can produce the same time or frequency offset over a given time interval. It does not indicate whether the time or frequency is right or wrong but only whether it stays the same while accuracy indicates how well an oscillator has been set on time or frequency. The frequency/phase instability is

categorized into two forms: short term and long term instability. Short term instability usually refers to fluctuations over intervals less than 100 s and is due to instantaneous frequency variation around a nominal center frequency. Long term instability can refer to measurement intervals greater than 100 s, but usually refers to periods longer than one day and is caused by a change in average or nominal center frequency. It describes the slow change of clock signals from nominal value over time. Stability estimates can be made in either the frequency domain or time domain and can be calculated from a set of either frequency offset or time interval measurement. Non classical statistics is often used to estimate stability in the time domain. This statistics is called Allan variance or Allan deviation. Figure 2.7 shows the sample phase plot for variation of frequency with time (Vig, 2004).

a) Unstable and not accurate   b) Stable but not accurate

c) Accurate but not stable   d) Stable and accurate
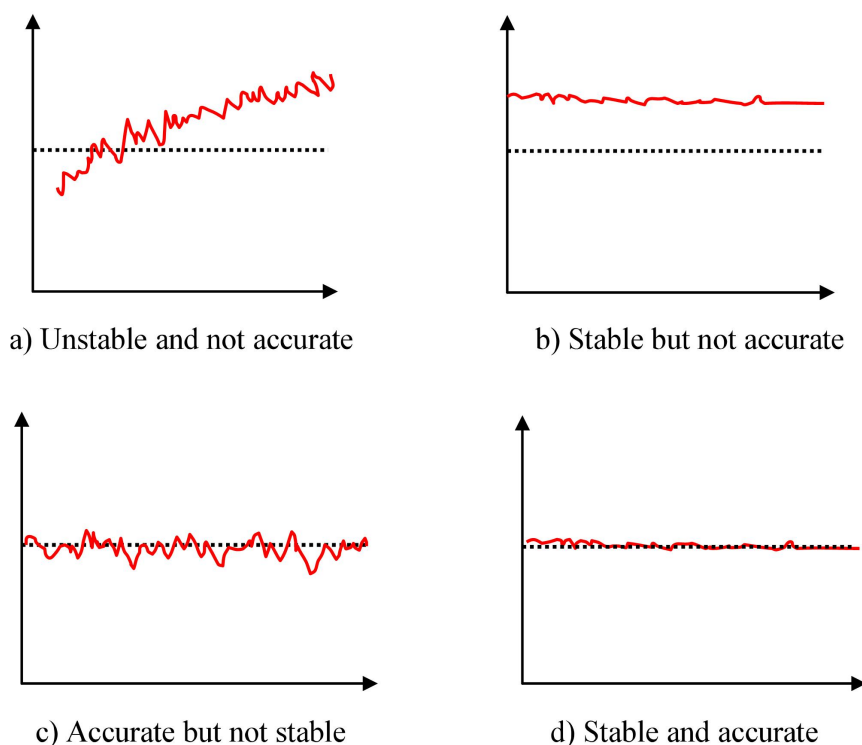
Figure 2.7: Relationship between stability and accuracy.

2.5.2 Phase Noise Measurement

Phase noise is generally considered the short term phase/frequency fluctuation of an oscillator or other RF/microwave component due to different noise sources. Measurements such as short term frequency (phase) instability and long term instability can be done. Phase noise measurement is a method of characterizing the stability of a frequency source and is done by directly measuring phase fluctuations and is useful for determining the short term stability of the signal that is to be used for synchronization of various system components. Figure 2.8 shows the plot for real low noise signal generators.
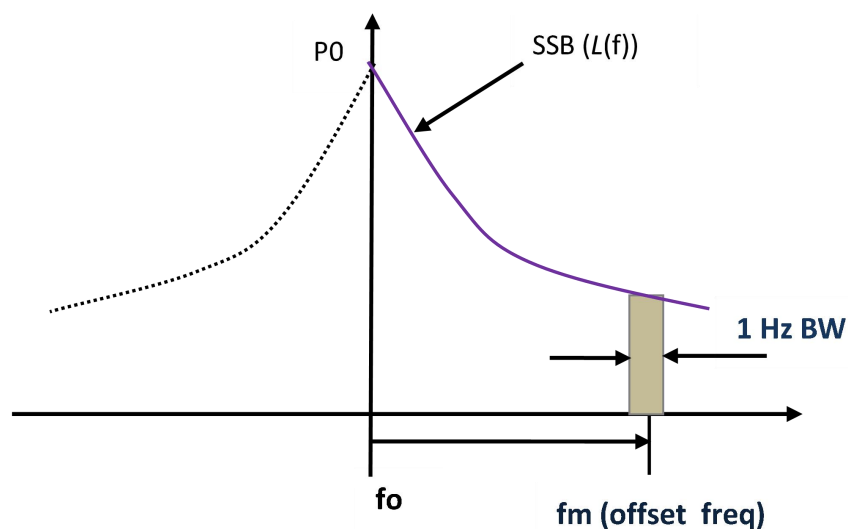
Figure 2.8: Plot for real low noise signal generator

When measuring phase noise measurement, the signal at a specific offset is measured as the relative power of the signal in a normalized 1 Hz bandwidth compared to total signal power. The signal level in dBc/Hz can be directly related to the amount of the phase disturbance the noise generates in that narrow band of modulation frequencies. The phase noise at a given offset expressed in dBc/Hz can be directly translated into degrees or radians in a one Hertz bandwidth independently of the offset frequency. All sources of noise can be converted to the equivalent phase modulation factor

regardless of whether they are caused by direct modulation of the source (e.g are truly phase modulation) or are added by some other method (e.g frequency modulation, added white noise). Phase noise is the noise sidebands around the delta function representing a perfect oscillator at a fixed frequency that would expect from theory.

Phase noise is commonly measured using spectrum analyzer. By measuring the total carrier power and then measuring the noise signal at a specified offset of the carrier, a phase noise measurement can be achieved.

2.5.4. Allan Variance

Characterization of the instability of the frequency source involves determining how the measured fractional frequency fluctuations of the source vary as a function of the time over which the frequency is average and is commonly expressed using Allan deviation. The Allan Variance or two sample Variance was first introduced by David W. Allan for the evaluation of the stability of time and frequency standards (Jespersen, 1970). The main idea behind this method lies in the relation of the dispersion that a set of measurements has, with the noise we expect to find in the output signals. The most common measure of dispersion is the classical variance, whose value decreases as the number of data points included in the calculations, increases. Allan deviation, σ_y (τ) can be computed from a series of consecutive frequency measurements, each obtained by averaging over a period τ. This averaging time corresponds to the gate time of a frequency counter used to make the frequency measurements (Sullivan, 1990; Walls, 2001). To compute σ_y (τ), we introduce some definitions.

The Allan deviation for an averaging time τ is then defined as

$$\sigma_y(\tau) = \left\langle \frac{1}{2}\left[\bar{y}(t+\tau) - \bar{y}(t)\right]^2 \right\rangle^{1/2} \tag{2.22}$$

where $\langle \; \rangle$ indicates an infinite time average and $\bar{y}$ represents the time average of y(t) over a period τ. The $\sigma_y(\tau)$ can be estimated from finite set of N consecutive average values of the center frequency, v_i, each averaged over a period τ.

$$\sigma_y(\tau) = \left[\frac{1}{2(N-1)v_0^2}\sum_{i=1}^{N-1}(\bar{v}_i - \bar{v}_{i+1})\right]^{1/2} \tag{2.23}$$

The Allan deviation is useful for characterizing a frequency source because the type of phase noise present is revealed by how $\sigma_y(\tau)$ depend on τ. For example, if $\sigma_y(\tau)$ is proportional to τ^{-1} then white phase noise present is the dominant noise process, whereas if $\sigma_y(\tau)$ is proportional to $\tau^{-1/2}$ then white frequency noise is dominant (Barnes, 1971; Witt, 2005). Allan deviation graph shows that stability of the device improves as the averaging period gets longer since some noise types can be removed by averaging. At some point, however, more averaging no longer improves the results. This point is the noise floor or the point where the remaining noise consists of non stationary processes such as flicker noise or random walk. There are five noise types namely; white phase, flicker phase, white frequency, flicker frequency, and random walk frequency as shown in Figure 2.12 (Walls, 2001; Emilie, *et. al.*, 2006). The gradient of the Allan deviation curve can be used to identify the amount of averaging required to eliminate noises types. The five noise processes from the log-log plot of

non-overlapping Allan deviation as a function of averaging time are shown in Figure

2.9 (Rutman, *et. al*, 1991; Walls, 2001; Emilie, *et. al.*, 2006).
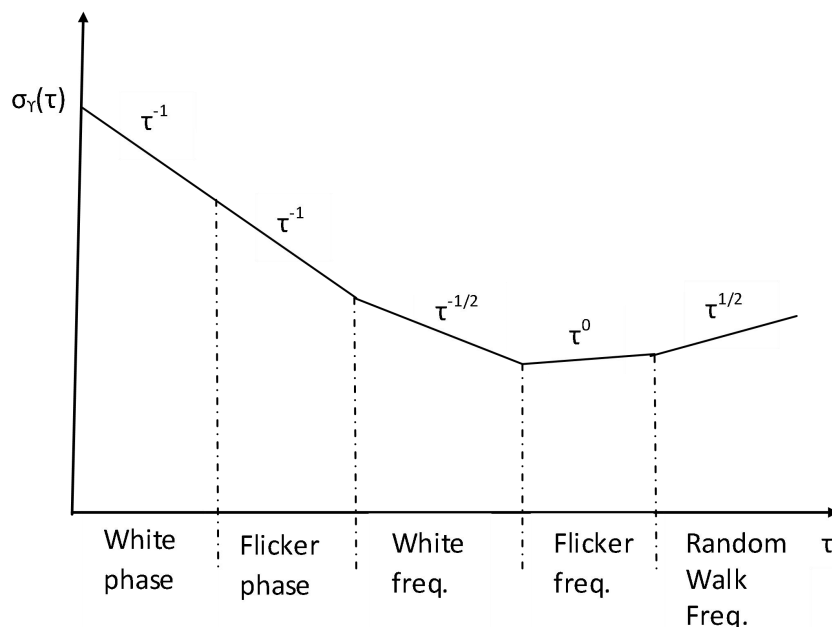
Figure 2.9: Allan deviation as a function of averaging time

Using data from a set of stability graph shows phase plot dominated by white noises

(1 s averages), white frequency noise (64 s averages), flicker frequency noise (256 s

averages), and random walk frequency (1024 averages).

Random walk frequency is noise close to the carrier and is difficult to measure. It is

usually related to the oscillators physical environment (mechanical shock, vibration,

temperature, or other environmental effects). If a random walk of frequency is the

dominant feature it may cause random shifts in the carrier frequency. Flicker FM

(flicker of frequency) noise is typically related to the physical resonance mechanism

of the active oscillator or the design or choice of parts used for the electronic or power

supply, or even environmental properties. The time domain frequency stability over

extended periods is constant. In high quality oscillators, this noise may be marked by

white FM of flicker phase modulation. White FM (white frequency, random walk off phase) is a common type of noise found in passive resonator frequency standards. Cesium and rubidium frequency standards have white FM noise characteristics because the oscillator is locked to the resonance feature of these devices. This noise gets better as a function of time until it becomes flicker FM noise. Flicker phase is noise related to physical resonance mechanism in an oscillator. It is common in the highest quality oscillators. This noise can be introduced by noisy electronics-amplifiers necessary to bring the signal amplitude up to a usable level and frequency multipliers. This noise can be reduced by careful design and by hand selecting all components. White FM (white phase) is generally produced in the same way as flicker FM. The late stages of amplification are usually responsible for white phase noise. This noise can be kept low by careful selection of components and by narrow band filtering at the output.

2.6 System Performance

Overall system performance of a communication link can be analyzed using bit error rate (BER) and eye diagram as a function of the receiver sensitivity. Receiver sensitivity relates the amount of optical power needed to obtain the minimum BER. BER parameter determines the transmission distance of an optical communication system. To transmit signals over long distances, it is necessary to have low BER (Hossain, *et. al.*, 2015).

2.6.1 Eye-Diagram Analysis

The eye-diagram technique is a simple but powerful measurement method for assessing the data-handling capability of a digital transmission system. Simulation platform uses eight different 3-bit long combinations to simulate the eye diagrams.

The output of each is overlapped and hence the eye diagram. Figure 2.10 shows an eye diagram with the major features.
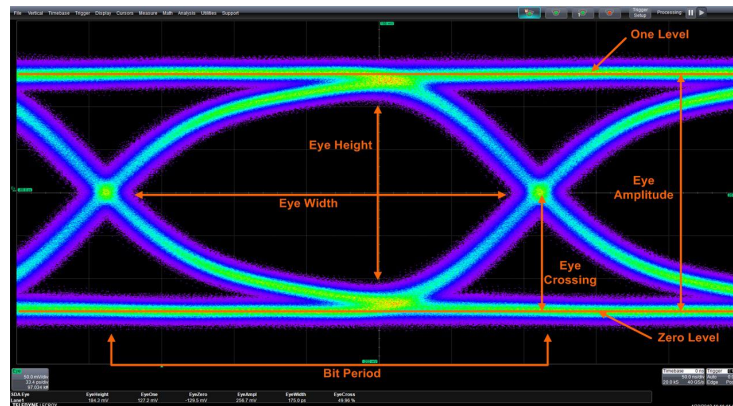
Figure 2.10: Eye diagram with main features marked.

The main measurement parameters associated with eye diagrams include bit period, zero level, one level, eye amplitude, eye height, eye width and eye crossing. Vertical eye opening indicates the amount of difference in signal level that is present to indicate the difference between a one and a zero bit. The bigger the difference the easier it is to discriminate between one and zero. Whereas, horizontal eye opening indicates the amount of jitter present in the signal, an open eye pattern corresponds to minimal signal distortion. As the transmission bit rate increases, the eye opening reduces to a limit where the eye does not exist anymore. Distortion of the signal waveform due to inter symbol interference and noise appears as the closure of the eye diagram. Due to the indecisive decision level, it is impossible for the receiver to decode the optical signal correctly. The performance probability related to this is known as the bit error rate (BER). Thus, the performance of a laser source is limited by the transmission rate. Thus, the system performance of an optical transmitter measured by eye-diagram technique is limited by the laser rise time constant as well

as the choice of line coding. Clearly open eye diagrams signify low noise or no distortions and thus imply higher signal quality.

2.6.2 Bit Error Rate

Bit error rate (BER) is the ratio of the number of bit errors detected in the receiver to the number of bits transmitted. For example, a transmission having a BER of 10^{-9} means that out of 1,000,000,000 bits transmitted one bit is an error. An error can occur as a result of an incorrect decision being made in the receiver due the presence of noise on a digital system. The decision to sample and whether the sampled value represents a binary 1 or 0 is affected by noise and signal distortion in the real system and there is a nonzero probability of an erroneous decision. Therefore, the received signal quality is directly related to the BER, which is a major indicator of the quality of the overall system. Monitoring the quality of an optical signal is fundamental in achieving reliable and effective communication in a high speed optical link. The quality of the signal degrades as it propagates along the fibre due to transmission impairments along the link. During data transmission in an optical communication channel, there are possibilities of errors being introduced due to linear and nonlinear effects. If errors are introduced into the data signal, then the integrity of the system is compromised. The BER is the most reliable and conclusive optical signal quality determinant in a high speed optical communication channel (Bondurant, and Atia, 1999; Lyle, and Anderson., 1994; Liu, and Wei, 2002). In digital transmission, the data stream can be altered due to attenuation, noise, dispersion, crosstalk between adjacent channels, distortion or synchronization errors. Its performance may be improved by launching a strong signal into a transmission system.

$$BER = \frac{1}{2} erf\left(\frac{Q}{\sqrt{2}}\right) \approx \frac{\exp\left(\frac{-Q^2}{2}\right)}{Q\sqrt{2\pi}} \qquad\qquad (2.24)$$

The error floor at an acceptable BER threshold is of order of 10^{-9} without compensation. In order to transmit signals over long distances, it is necessary to have a low BER and high Q factor within the fibre (Hossain, *et. al.*, 2015). On-off keying (OOK) method gives a fairly good prediction of BER, although noise distribution in the intensity domain is not exactly Gaussian (Azizoglu and Humblet, 1991).

2.7. Review of Stable RF Dissemination Systems

Stable frequency sources play an important role in many modern metrology and fundamental physics applications. High sensitivity is required in transmission systems and thus, low noise and stable oscillators and clocks are employed. However, optical transmitters, receivers and passive components add some instabilities that degrade system performance resulting in instabilities in the system. As a result, there is a demand to obtain a simple and cost effective system for distributing reference frequency which is stable and accurate.

Demand for simple and cost effective system for distributing stable reference frequency is being explored. A challenge in the distribution of coherent frequency sources is in the transmission of coherent signal, over long distances, with minimal perturbation. The traditional solutions for long-haul time and frequency (T&F) transfer are based on satellite techniques that use either global navigation satellite systems (GNSS) or geostationary satellites (Lewandowski, *et. al.*, 1999; Petit *et. al.*, 2008; Piester *et. al.*, 2008). This method is used to compare the frequency and time standards of national laboratories around the world. In this scheme, the transmitter

and the receiver both compare their times simultaneously with that of a common global positioning satellite (GPS). The satellite T&F transfer is widely accessible but does not allow to exploit the actual accuracy and stability of the best atomic clocks and timescales at the remote end. Considering the complexity and cost, it is desirable to implement frequency transfer over the existing wide-spread fibre-optic telecom networks.

Frequency standards based on optical transitions in various atomic systems provide the potential for developing optical atomic clocks in the near future that are several orders of magnitude more stable than the best existing clocks based on microwave frequency references. The excellent stability that will be provided by optical clocks, and even the stability they currently offer, has applications in several fields, ranging from studies of fundamental physics to communication and remote synchronization. However, since optical clock systems are too complex to be portable, these applications rely on the ability to transfer over several kilometres a stable frequency reference that is linked to an optical clock. Clock signals in the network will be required for phase coherence, the absolute time code for antenna controllers and beam formers, accurate timing ticks and counters for data stamping, synchronization, operational monitoring and control (Peens-Hough, 2012). Initial research oriented systems were complex and not portable. The ability to remotely transfer frequency reference without introducing any additional instability is of great concern and urgent for optical clock development.

An extremely promising alternative for stable distribution of a frequency reference is transmission over the fibre. The frequency reference either optical or microwave is encoded onto an optical carrier for transmission over a fibre network. Remote users

are then able to recover the frequency reference by decoding the received optical signal. It has been shown that optical fibre has the potential to disseminate stable radio-frequency (RF) signal over long distance due to its low attenuation, high reliability, and immunity to electromagnetic interference (Narbonneau, *et. al.*, 2006). Jet Propulsion Laboratory paved the way for the development of a fibre based distribution system for the NASA Deep Space Network (Primas, *et. al.*, 1988; Logan and Lutes, 1992). In astronomy, modern telescope synchronization like the Atacama Large Microwave Array (ALMA) relied on optical fibre for transmission (Sato *et. al.*, 2000). While the National Institute for Standard and Technology (NIST) have been connected with JILA using high performance optical link (Holman, *et. al.*, 2004). Fibre based frequency dissemination has achieved significant progress in; ultra stable frequency dissemination over urban fibre link (Williams, *et. al.*, 2008; Fujieda, *et. al.*, 2011; Predehl, *et. al.*, 2012). Time and frequency synchronization network has been demonstrated (Bai, *et. al.*, 2013; Zhang, and Zhao, 2015), based on dissemination frequency. The schemes can be divided into optical frequency dissemination and radio frequency dissemination (Wang, *et. al.*, 2012; Lopez, *et. al.*, 2013; Zhang, and Zhao, 2015; Krehlik, *et. al.*, 2015). Ultra long distance frequency dissemination under single span stabilization mode has been realized via optical frequency dissemination. This is because the linewidth of disseminated optical frequency is a few hertz (Hz) range. Due to long coherent length and low CD effect, ultra long distance dissemination can be realized by adding several amplifiers along the fibre route.

For RF modulated frequency dissemination, the laser carrier has a large spectral width. The accompanying CD effect limits the dissemination distance which leads to large BER. In fibre optic communication, transfer distance at a certain data rate is often

given by lasers dispersion tolerance. Low modulation frequency leads to longer transfer distance but cannot achieve high dissemination stability due to its low phase resolution (Krehlik, *et. al.*, 2015). Consequently, for longer distance, cascaded frequency dissemination is the best choice, meaning disseminated frequency has to be demodulated and remodulated again using cascaded frequency stabilization system. Long term continuous frequency dissemination which give stability at the integration time of 10^6 s has been reported using only RF modulated frequency dissemination method (Śliwczyński, *et. al.*, 2011). Simultaneous time and frequency synchronization is also realized via RF modulated method (Wang, *et. al.*, 2012) and this has currently a number of practical application like deep space navigation (DSN) and radio telescope array. Optical fibre also provides a means for remote comparison between highly accurate time and optical-frequency standards. For example, transfer of repetition rate of highly stable mode-locked laser pulses (Marra, *et. al.*, 2012), comparisons of optical-clock over a 920-km fibre link (Predehl, *et. al.*, 2012) and a 540-km fibre-optic network carrying internet traffic (Lopez, *et. al.*, 2012, 2013). A continuous frequency transfers with an accuracy of 5×10^{-19} / day over an 80-km fibre optic link has also been reported (Wang, *et. al.*, 2012). In other studies, transfer of a clock signal together with data traffic has been reported (Kefelian, *et. al.*, 2009; Lopez *et. al.*, 2010), using a high gain amplifier for a long-haul link. Transfer solutions of Radio-frequency (RF) reference signal at 10 MHz and 100 MHz have been proposed (Krehlik, *et. al.*, 2016; Lopez, *et. al.*, 2012). Moreover, optical carrier transfer techniques have been developed to observe the relative frequency stability of optical clocks and cavity stabilized lasers (Terra, *et. al.*, 2009; Pape *et. al.*, 2010). Furthermore, the introduction of a system that simultaneously transmits stable RF signal and data is a novel technology in transmission systems. The development of

long-distance, high-resolution frequency transfer is an important issue, in remote clock synchronization and comparison, Astrophysics long baseline interferometers and deep space network benefits from such frequency transfer system. Performance of VCSEL and DFB laser on a 1 kHz and 10 kHz clock signal has been investigated (Rotich, *et. al.*, 2017). Wavelength shifting of a modulated laser is one of the main factors limiting long term stability of time and frequency output signals (Śliwczyński, *et. al.*, 2013).

2.8 Modulated Raman Pump in VCSEL Technology for Simultaneous Data and Clock Distribution

Raman amplification is a key technology for improving the performance of fibre optic transport systems. VCSELs on the other hand provide an attractive feature for use in optical frequency networks. In particular, their relatively low cost, low drive currents, energy efficiency, high bandwidth and wavelength tuneability make them ideal for on-site deployment (Olmos, *et. al.*, 2012; Larsson, *et. al.*, 2018). However, VCSEL technology is still limited by their low output optical power and frequency chirping resulting from dispersion effects within the fiber transmission length, therefore limiting the total attainable reach. To extend the transmission reach of VCSEL-based links for adoption in long haul networks, such as large-base interferometers, a proper signal amplification technique has to be adopted. Raman amplification is a promising approach to reach extension in terrestrial optical fiber networks. This is due to the possibility of achieving a high flat gain over a wide range of wavelengths, and the ability to achieve distributed Raman gain on any transmission fibre (Isoe, *et. al.*, 2014). The main motivation for using Raman amplification to boost the VCSEL is the broad bandwidth, high saturation input power and low noise figures (Pelouch, 2016).

Combination of VCSEL technology with Raman amplification is suited for long reach extension for wide area optical networks. This scheme can be used for duplex unidirectional and bidirectional data and clock distribution using forward and backward Raman pumping schemes respectively. Using a single fibre, it is possible to transmit data and clock concurrently. Raman pump can be utilized to amplify VCSEL data and modulated to transmit clock signal. Advancements in semiconductor lasers and receiver technologies have led to the adoption of VCSELs in reference frequency (RF) distribution systems (Rotich, *et. al.*, 2017). Long-haul RF distribution networks are characterized with longer baselines (over 100 km), which need an intelligent dispersion management mechanism to achieve its observational objectives. This can be implemented by exploiting high speed VCSELs in RF clock signal transmission, and Raman amplification in dispersion management to maximize the transmission reach.

Combined optical/RF and data dissemination system that offer higher stability is being explored. The technique for maximizing carrier spectral efficiency and extending transmission reach through combined adoption of VCSELs, four level pulse amplitude modulation (4- PAM), dense wavelength division multiplexing (DWDM) and Raman amplification has been reported (Isoe, *et. al.*, 2018). Long reach transfer of accurate 2 GHz reference frequency clock signal for extended reach RF distribution has been demonstrated using distributed forward Raman amplification (Isoe, *et. al.*, 2019). Integration of Raman amplification and VCSEL-based RF clock signal transmission is a viable alternative approach for maximizing reach in the next-generation timing and frequency distribution systems. In extending reach to meet the unique requirements of terrestrial fiber networks, such as telescope array networks

with longer base-lines, Raman amplification has been adopted. Raman pump in the counter scheme was used to successfully transmit a 10 kHz clock signal while amplifying the VCSEL's data signal (Rotich, *et. al.*, 2017). Backward pumping offers an important feature of bidirectional duplex data transmission a technique that can be employed in hyper-scale data centers to simultaneously send and receive data in the next generation ultra high speed data transmission for ultra-long haul networks and wide area networks (WAN).

CHAPTER THREE

METHODOLOGY

3.1 Introduction

This study involved data collection and analysis from several experimental setups. All the experiments were done at the centre for broadband communication, an ultra-modern laboratory at Nelson Mandela University, Port Elizabeth-South Africa. In this chapter, the setup for each experiment is presented.

3.2 Experimental performance evaluation of VCSEL transmission

Transmission capability of a 10 Gbps VCSEL was experimentally investigated using the setup in Figure 3.1. A 1550 nm VCSEL laser was directly modulated with data and coupled into the device using bias tee (BT).
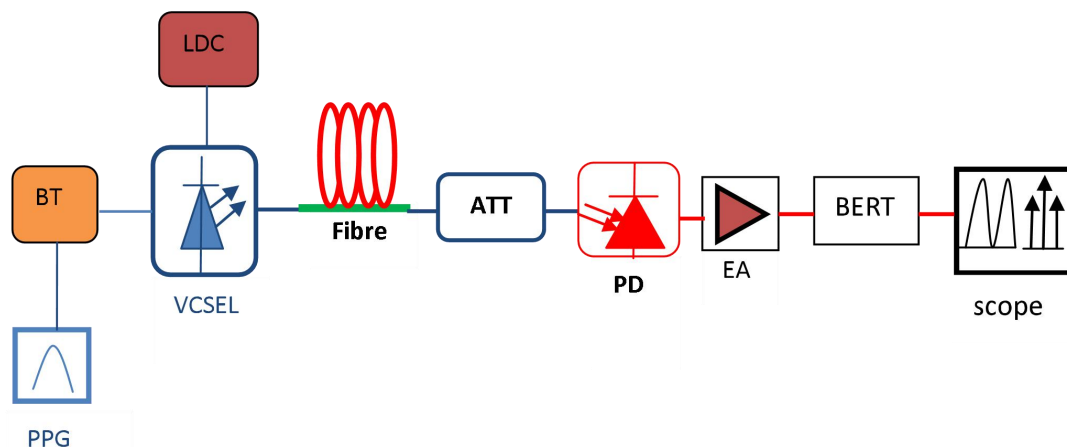

Figure 3 .1: Experimental setup for VSCEL data transmission.

The laser diode controller (LDC) was used to adjust bias current being injected to the laser. The VCSEL was directly modulated with a 10 Gbps pseudorandom binary sequence (PRBS) data signal of length 2^7-1 from a programmable pattern generator (PPG). The modulated signal was then launched into a standard single mode fibre

(SMF-Reach) of length 24.69 km for transmission. Attenuator (ATT) was used to vary optical power at the receiver. Optical power was varied to establish bit errors at different power levels. VCSEL transmission performance was analyzed by varying the power getting into the photodiode (PD) receiver to measure bit error rate (BER) at different bias current. Electrical amplifier (EA) amplifies the received signal to meet the required operating voltage for bit error rate tester (BERT). BERT determines the number of bit errors in transmission. BER measurement in data transmission is used to compare the quality of different systems for data transmission. The scope was used to analyse eye diagrams at different bias current.

3.3 Experimental setup for demonstrating Raman amplification in VCSEL technology employing different pumping schemes.

Figure 3.2 shows the experimental setup used to demonstrate Raman amplification and VCSEL-based Raman assisted long reach data distribution system. Raman amplification using a weak signal from un-modulated VCSEL laser with an output power of -10.14 dBm and a 1450 nm Raman pump was first demonstrated. A Raman pump from JDSU model number 34-GVT- was used. The Raman pump used operates at 1450 nm region providing maximum amplification at 1550 nm window. Two pumping schemes were employed in the study that is; forward pumping and backward pumping. Forward pumping was achieved by switching on Raman pump 1 and switching off Raman pump 2. Backward pumping was realized by switching on Raman pump 2 and switching off Raman pump 1. The on-off gain was obtained for different pump powers, fibre length and input signal for the two pumping schemes. The demonstration employed Raman amplification and VCSEL technology to transmit data over 50 km.
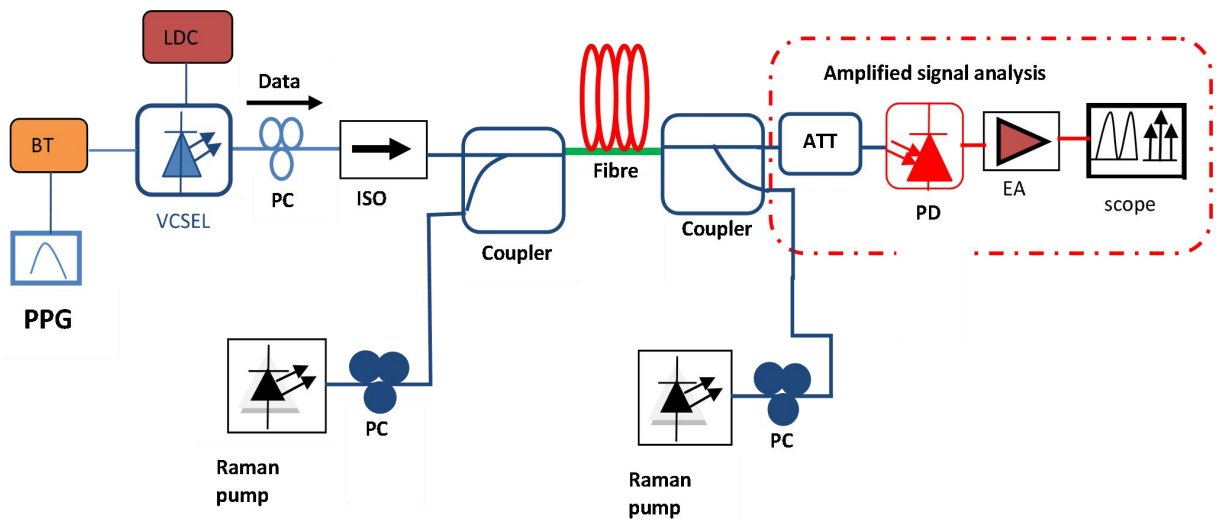
Figure 3.2: Experimental setup for Raman amplified in VCSEL data transmission system.

A 1550 nm VCSEL laser with an output power of -10.14 dBm and a 1450 nm Raman pump were used in this experiment. The VCSEL laser was modulated with a 10 Gbps pseudorandom bit sequence (PRBS) electrical signal pattern of length (2^7-1). For maximum power output the polarization controller (PC) was used to adjust polarization of the signal. The isolator (ISO) was used to protect VCSEL laser from backward pump power. The signal and pump were coupled into the fibre using a 1450 nm/1550 nm optical coupler and propagated through a 50.7 km single mode fibre. The weak signal from the VCSEL was amplified during transmission in the fibre resulting in the signal gain. An Attenuator (ATT) was used to vary optical power at the receiver. A PD was used to recover the transmitted data for BER measurement and eye diagram analysis. The EA amplifies the received signal while the scope analyses the eye diagram. Effect of backward and forward Raman pumping schemes on transmitted data was analyzed.

3.4 Experimental demonstration of Raman Assisted-VCSEL for Enhanced Full-Duplex Bidirectional/Unidirectional Data Transmission with modulated Raman pump signals

Figure 3.3 shows the experimental setup used to demonstrate bidirectional and enhanced duplex data transmission using VCSEL and Raman laser simultaneously over 50.7 km True-wave Reach fibre from OFS Furukawa company.
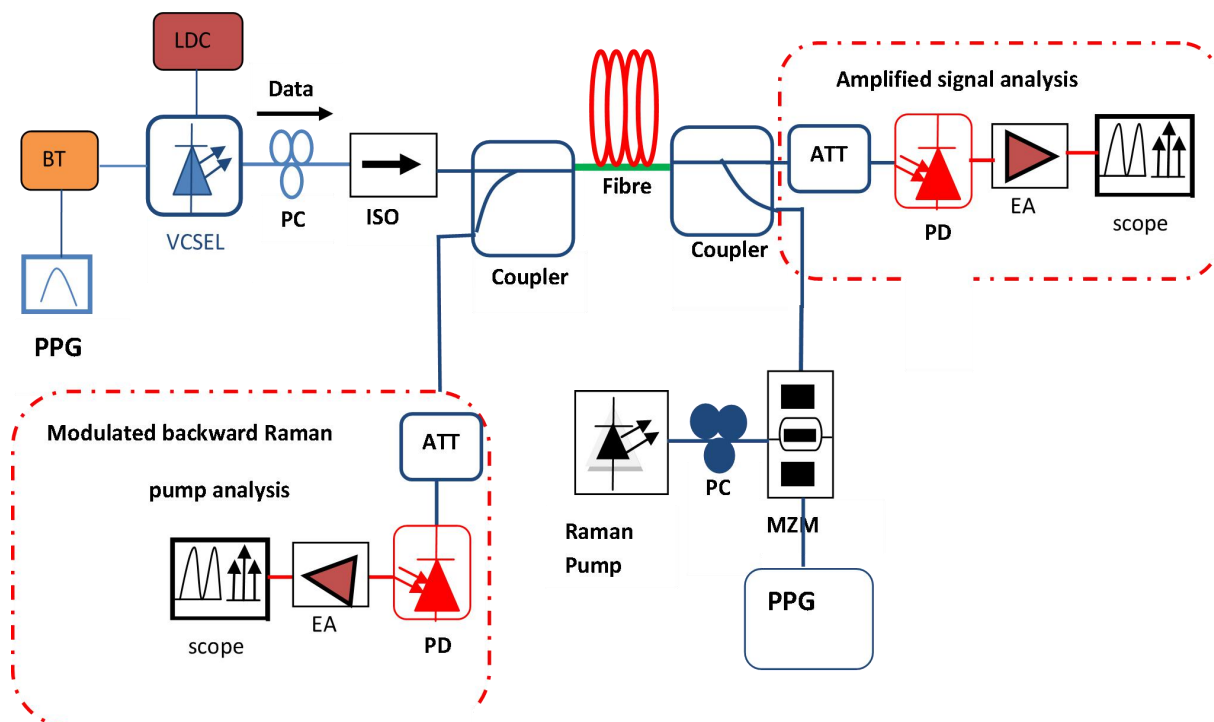
Figure 3. 3: Experimental setup for simultaneous bidirectional duplex data transmission

True-wave Reach fibre is compliant to both G.655 and G.656 fibres. The 1550 nm VCSEL laser was directly modulated with 8.5 Gbps electrical signal from Pseudorandom bit sequence generator of pattern length 2^7-1. A single ended output bit error rate tester (X-BERT) was used to generate the electrical signal. The X-BERT used had a reference clock frequency ranging between 531 and 707 MHz, with a pattern invert ability available for all patterns and an 8B10B encoding for precisely

accurate clock recovery and BER computation. Raman pump of center frequency 1450 nm was modulated externally using Mach-Zehnder modulator (MZM) with 8.5 Gbps data. A 8.5 Gbps data from signal generator was fed to the VCSEL through a bias tee (BT). The VCSEL signal was counter-propagated with the modulated Raman pump in the fibre. To realize enhanced bidirectional data transmission modulated Raman pump with an output power of 20.34 dBm was counter-propagated with the signal resulting to signal amplification. The transmitted Raman pump signal carrying data was received by a second PD for analysis. VCSEL signal transmission with un-modulated Raman was demonstrated first followed by VCSEL transmission with modulated Raman by looking at the eye diagrams and BER analysis.

The analysis for enhanced VCSEL transmission with backward pumping and modulated Raman transmission show the technique for full duplex data transmission. The scheme was used because it is attractive and only a single fibre was required to transmit data simultaneously from both ends. Raman pump was utilized twice, that is, amplifying VCSEL signal and modulated to transmit data over 50.7 km. Unidirectional VCSEL transmission over extended reach network was obtained by using forward pumping where the Raman pump coupled with the transmitted signal from the transmitter end. A sensitive PD of bandwidth 10 GHz was used to recover the transmitted data. The EA was used to amplify the signal to be detected by Scope analyzer for pattern and eye diagram analysis. Polarization (PC) were used to orient the states of polarization of the signal and pump wavelengths to ensure the best The transmission performance of the VCSEL channel was accurately measured in real time without Raman pumping and with forward and backward Raman pumping over a 50.7 km fibre link. After attaining a successful error-free VCSEL-based Raman-

assisted transmission over the 50.7 km fibre link, maximizing the network efficiency was experimentally demonstrated. A 50.7 km of TrueWave Reach fibre from (Optical Fiber Solutions) OFS Furukawa company was used in this work. Eye diagram analysis and BER curves were obtained for the three different scenarios.

3.5 Experimental demonstration of Modulated Raman Pump for Integrated VCSEL-based Reach Enhancement and Clock Tone Dissemination in optical Communication

Figure 3.4 shows experimental setup used to demonstrate simultaneous 10 Gbps data transmission and reference clock signal dissemination over 50.7 km standard single mode fibre (SMF).
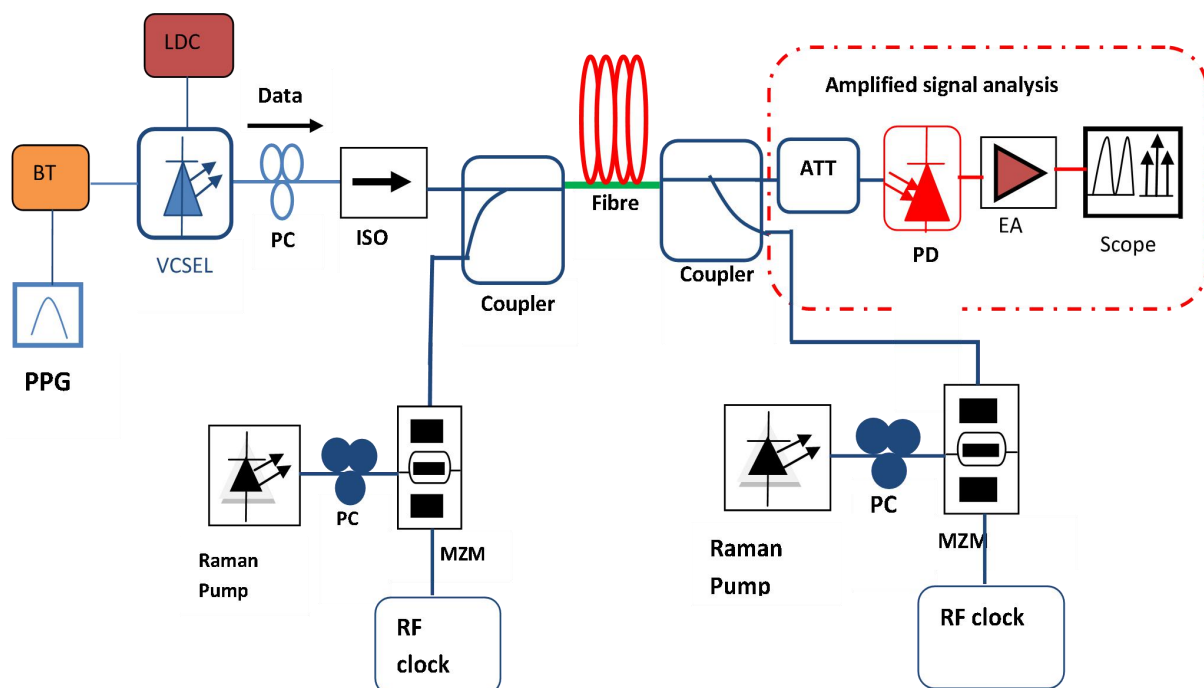

Figure 3 .4: Experimental setup for simultaneous transmission of data and clock signals

A 1550 nm VCSEL laser with an output power of -10.14 dBm at 7.04 mA bias current and a 1450 nm Raman pump laser diode were used in our experiment. PC controllers

were adopted to provide active polarization control for signal and pump wavelengths. VCSEL laser was modulated with a 10 Gbps pseudorandom bit sequence (PRBS) electrical signal of pattern length (2^7-1). A 1450 nm Raman pump with output power of 22.01 dBm was modulated by 2, 4, 6 and 8 GHz RF clock signal from signal generator via MZM. The signal wavelength was coupled with Raman pump wavelengths by a 1450 nm/1550 nm optical coupler and co-propagated into a 50.7 km fibre. At the receive end, the received optical signal was directed to a 1450 nm/1550 nm optical coupler to separate the signal wavelength from the pump wavelength for simultaneous analysis. A weak signal at the output of VCSEL co-propagated with Raman pump in the transmission fibre resulting to Raman amplification. The procedure is repeated for forward pumping where the weak signal counter-propagates with clock signal. A PD is used to recover transmitted data for BER measurement and eye diagram analysis. Also the clock is recovered using a PD for phase noise measurement employing direct method with an electrical spectrum analyzer. Raman pump was also utilized to transmit clock signal. A 50.7 km optical fibre was used to distribute optical signal and the effect it has on the phase stability of the clock was studied. The central frequency of 4 GHz RF clock signal was chosen to demonstrate simultaneous transmission of the clock and enhanced data. Phase noise and spectrum for different pumping schemes at 4GHz RF clock signal was measured and compared with electrical signal.

3.6 Experimental demonstration of DFB LASER in RF clock distribution

The schematic diagram for RF clock distribution system used is shown in Figure 3.5 below. The 1550 nm distributed feedback (DFB) laser was used to distribute RF clock signal over a 24.69 km single mode reach fibre (SMF-R). The DFB laser was

modulated with 2 GHz, 4 GHz and 6 GHz RF clock signal from a signal generator. The resultant 2, 4 and 6 GHz electrical signal after the PD, was measured with frequency counter resolution 100 mHz and analyzed using Rohdes and Schwarz (R&S) electrical spectrum analyzer (ESA).
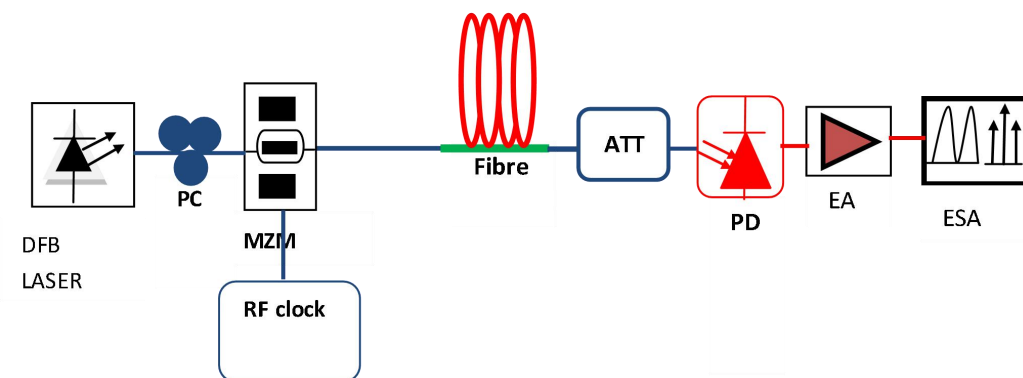

Figure 3 .5: Experimental setup for RF clock signal dissemination using modulated DFB laser

Frequency stability of the transmitted signal along the 24.69 km fibre link was experimentally evaluated and analyzed. Thereafter, the Allan deviation of the RF signal was computed using the computer based R&S Allan variance software.

CHAPTER FOUR

RESULTS AND DISCUSSIONS

4.1 Introduction

This chapter is devoted to report and discuss the experimental results. Sections 4.2 to 4.5 focuses on optimization of VCSEL and DFB lasers results, investigation of VCSEL technology in data transmission, demonstration of Raman amplification and effect of Raman amplification on VCSEL technology for enhanced data transmission. Integration of modulated Raman pump for data transmission and amplification of VCSEL data is focused on in section 4.6 and 4.7. Modulated Raman pump for integrated VCSEL-based Reach enhancement and clock tone dissemination in optical Communication is presented in section 4.8. Finally, section 4.9 focuses on the performance of DFB laser and Raman pump on transmitted RF clock signals.

4.2. Optimization of VCSEL and DFB lasers

Before choosing a laser for any optical communication system its characterization is important to determine the optimum working for the laser. The choice of the transmitter in data transmission is an important underlying factor for low cost optical network. Figure 4.1 shows the bias characterization curves of 1550 nm VCSEL and DFB that were used for its optimization. As shown in Figure 4.1 (a), a threshold current of 1.30 mA with a current rollover point of 9.60 mA was attained. The drive current also remained below 10 mA, therefore showing a good energy efficiency of the device. Energy efficiency is an attractive feature for large-scale deployments of VCSELs, particularly in densely packed optical interconnects. Above current rollover, output power of VCSEL reduced with further increase in current. At high power

output, the slope of the curve decreases because of junction heating. Lasing threshold obtained for DFB laser was 11mA as shown in Figure 4.1 (b).
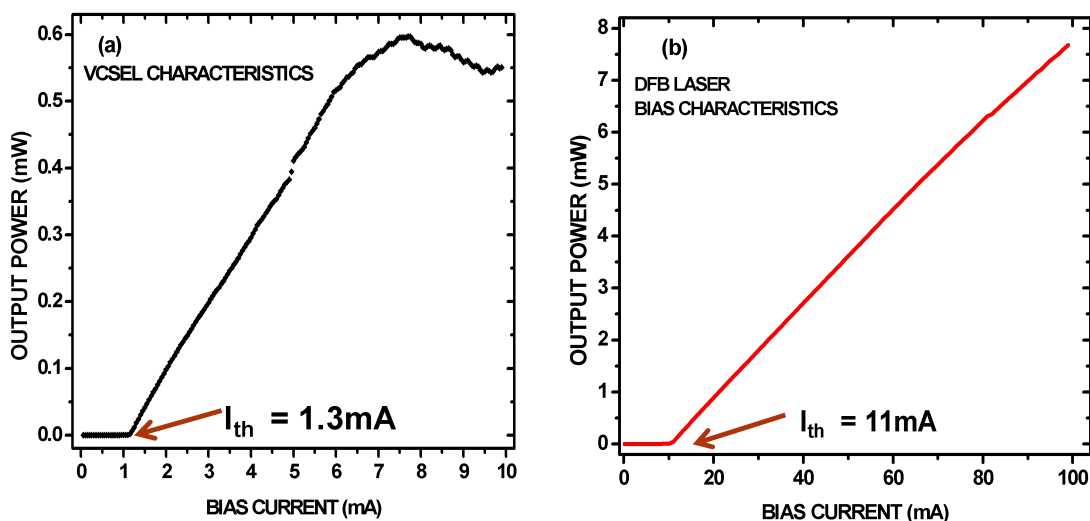
Figure 4.1: (a) Variation of output power with VCSEL bias current- lasing spectra at tuning currents of 0.05 mA to 9.90 mA. (b) DFB laser output power with bias currents from 0.05 to 99.05mA.

Results show that VCSEL is a low power laser compared to DFB thus suitable for low cost data transmission networks. Increasing bias current for VCSEL shifts the spectrum to longer wavelength as shown in Figure 4.2 (a). Wavelength tuning range of 8 nm was obtained by varying current from 2 to 9.50 mA. Figure 4.2 (b) shows a spectrum for DFB at 38.01 mA. The DFB laser exhibits stable single mode spectrum. For large-scale commercial installation of cost-effective high bandwidth optical fibre networks, low-cost, power and spectral efficient VCSEL technology is a viable approach.
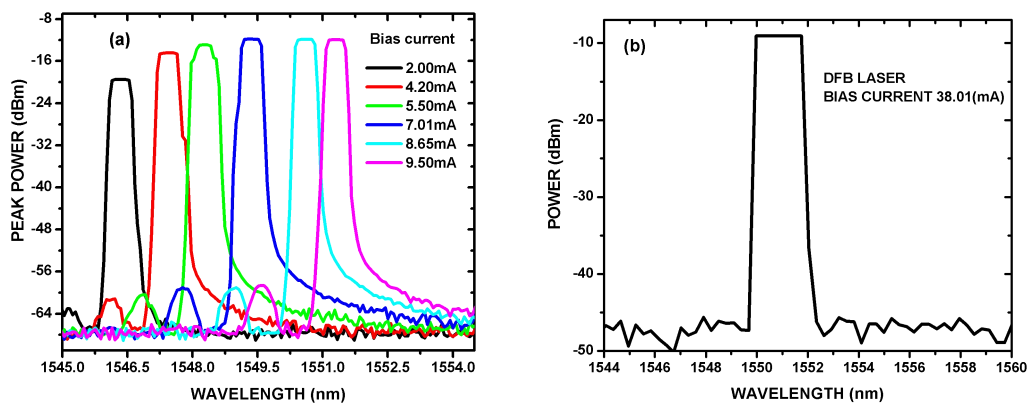
Figure 4.2: a) VCSEL wavelength tuneability with increasing bias current. b)Lasing spectrum for DFB laser at 38.01 mA.

This is due to their unique features such as low-power consumption, high-speed modulation with low drive currents and wavelength tuneability.

4.3. VCSEL technology in data transmission

Figure 4.1 and 4.2 shows that VCSEL laser requires low power and its wavelength can be tuned making it better data transmitter. BER measurement in data transmission was used to compare the quality of different systems for data transmission. Figure 4.3 (a) shows that receiver sensitivity increases with increase in bias current. Receiver sensitivities for bias currents of 4.85 mA, 7.04 mA and 9.09 mA are -18.4 dBm, -17.3 dBm and -16.9 dBm respectively at an acceptable BER threshold of order 10^{-9} without compensation.
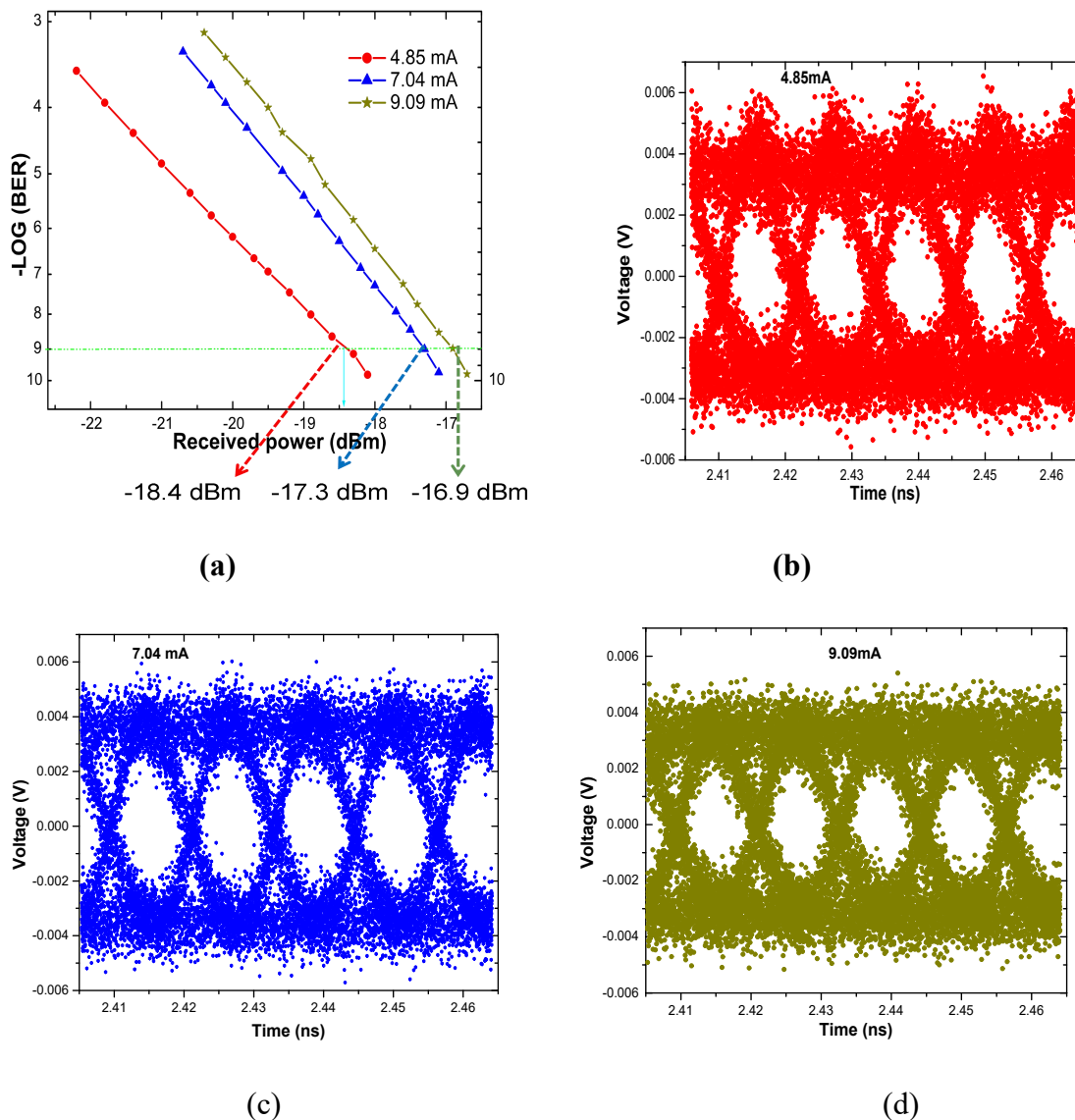
Figure 4.3: (a) VCSEL transmission performance at different bias current (b) Eye diagram at 4.85 mA (c) Eye diagram at 7.04 mA (d) Eye diagram at 9.09 mA.

Results shows that the transmission penalty increases with increase in bias current. Figure 4.3 (b), (c) & (d) indicates clearly open eye diagrams. Clear eye openings are observed for all bias currents, showing quality data transmission. The eye pattern measurements show the overall signal integrity of a data path. For optimal performance we biased the laser at 7.04 mA for subsequent experiments. Data transmission performance was analyzed by varying power getting into the Photodiode

receiver to measure Bit error rate (BER) at different bias currents. The data transmission was assessed by evaluating BER for B2B and 24.69km fibre.
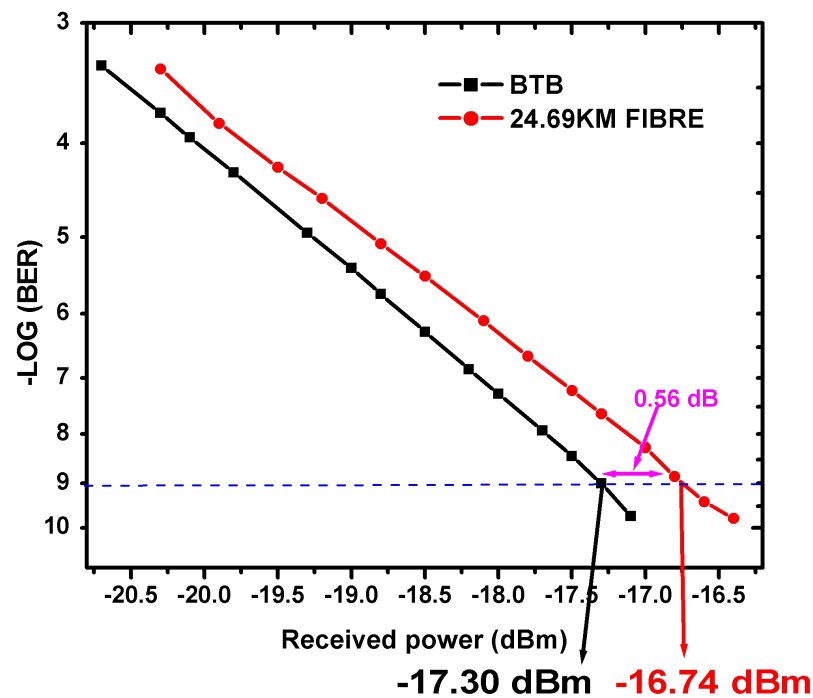
Figure 4.4: Variation of Log (BER) with received power for back to back (BTB) and 24.69 km fibre.

Back to back (B2B) transmission is achieved when the data is sent directly to the receiving end without propagating through a medium. The measured BER curves for B2B analysis and 24.69 km fibre transmission is shown in Figure 4.4. A receiver sensitivity of -17.30 dBm was obtained experimentally for B2B analysis and -16.74 dBm for 24.69 km fibre transmission. The fibre transmission introduced a penalty of 0.56 dB as shown in Figure 4.4 and this was contributed by losses in the fibre. Figure 4.5 shows clearly open eye diagrams for B2B and 24.69 km fibre. During transmission, however, the signal carrying data is attenuated hence need for enhancement.

Figure 4.5: Experimental measured eye diagrams for a 1550 nm VCSEL modulated at 10 Gbps: (a) transmission for BTB (black) (b) 24.69 km fibre (red).

Eye diagram provides visual information that is used to evaluate and trouble shoot digital transmission systems. When the eye is well open (clearly distinguishable) it means 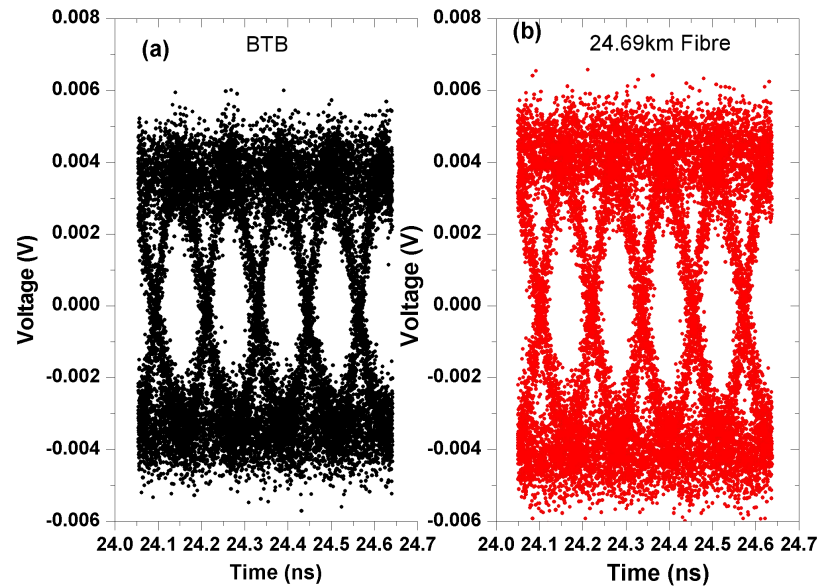transmitted bits are easily distinguished at the receiving end. The combination of frequency chirping and chromatic dispersion causes the eye diagrams closure. The eye diagram for B2B and one for 26.69 km are correlated indicating successful data transmission over the fibre. Chromatic dispersion and fibre nonlinearity are some of the constraints for error free data transmission over fibre. However, optical access networks require reliable, cheap and energy efficient broadband optical sources. VCSELs are suited for short distance data transmission and for 10 Gbps and above data transmission. However, they suffer from fibre dispersion and attenuation thus affecting their transmission performance over extended reach networks. Therefore, VCSEL require amplification to transmit over 50 km fibre while maintaining the integrity of the data transmitted.

4.4. Raman Amplification

Raman amplification is a non linear process where energy is transferred from the pump of shorter wavelength to a signal of higher wavelength through Raman process. Distributed Raman gain optimization in optical fibre networks is highly dependent on wavelength separation between the pump wavelength and the signal wavelength. Figure 4.6 shows the experimentally measured pump-signal wavelength separation.
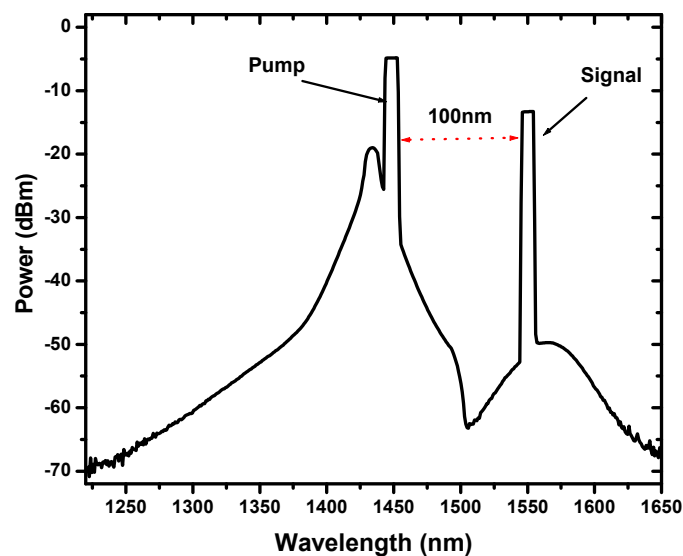
Figure 4.6: Raman pump signal wavelength detuning
It is evident from figure 4.6, that maximum gain was achieved when the pump wavelength is detuned 100 nm below the signal wavelength. It is important to note that Raman gain spectrum in standard single-mode optical fibres is extremely broad and extends over a wide range of wavelengths. There is increase in Raman gain when the wavelength difference between signal and pump increases and peaks at 100nm. The position of gain bandwidth can be adjusted by tuning pump laser wavelength.

Figure 4.7 shows the relationship between gain and input signal power. Raman gain is inversely proportional to signal power.
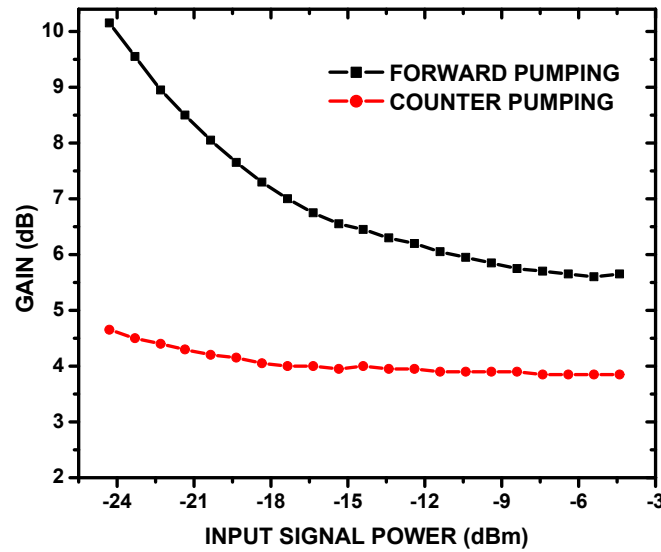
Figure 4.7: Relation between gain and input signal power

As signal power approaches the pump power, there is reduction in gain due to gain saturation. For forward pumping configuration gain is higher than backward pumping configuration since the signal interacts with the pump from the input of the fibre, hence more power is transferred to the signal. For counter propagation, the gain is lower because there is minimal interaction and the signal is attenuated more as it propagates through the fibre, thus lower gain. Amplification takes place when power is transferred from the pump to the signal. Reducing signal power while maintaining pump power, means the difference increases hence pump transfers energy to the signal resulting in more gain. The Raman on–off gain of the signal at different pump powers is shown in Figure 4.8 (a) and (b). On–off gain here refers to the difference between the signal power at the receiver end when the Raman pump laser diode is on and when off. The experimentally measured VCSEL-based Raman on–off gain for forward pumping and backward pumping schemes was attained by exploiting VCSEL tuneability.

Figure 4.8: **Variation of on-off gain with input pump power for a) 25.25 km b) 50.48 km Truewave fibre.**
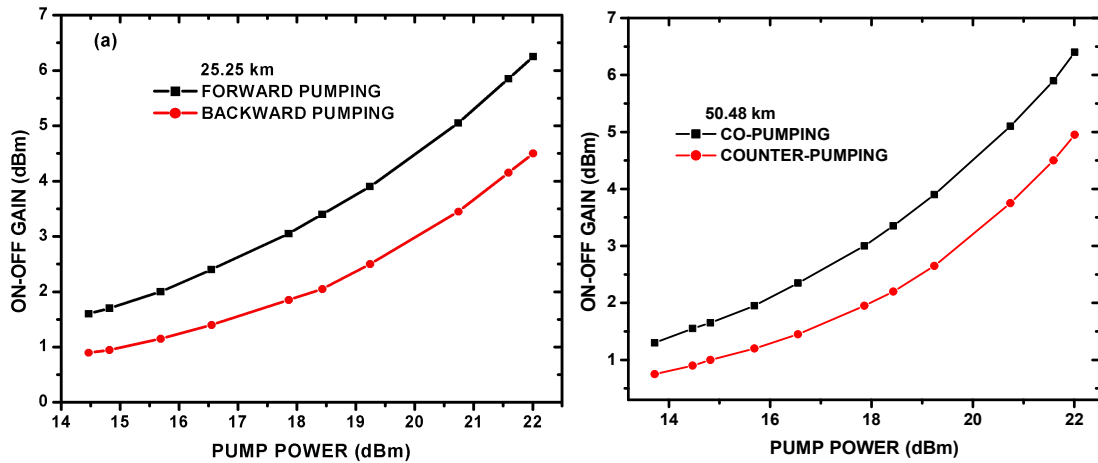
A signal power of −10.14 dBm and an SMF Reach fibre of length 25.25 km and 50.48 were used. As depicted in Figure 4.8, Raman gain was noted to increase with an increase in pump power for both pumping schemes. This is because as the pump power is increased, the relative power difference between the pump and the signal also increases, thus the pump transfers more energy to the signal resulting in more Raman gain. The maximum gain of 6.3 dB and 4.5 dB was obtained for forward and backward pumping respectively at 25.25 km and 6.5 dB and 5.0 dB at 50.48 km on a -10.14 dBm signal by using a 22.01 dBm pump power. From results in Figure 4.8, forward pumping was noted to have a superior Raman gain performance as opposed to backward pumping. Forward pumping has higher gain than backward because of enhanced signal-pump interaction. At the coupling end, the pump and the signal are relatively strong and both get weaker towards the end of the fibre. It is true that when a pump wavelength is co propagated with a signal wavelength, more pump energy is transferred to the weak signal, and thus, higher amplification levels can be achieved due to proper utilization of the pump power. This is due to the fact that both the pump

power and the signal power propagate in the same direction and the forward pumping ratio remains almost the same for forward pumping leading to more power transfer to the signal. Much pump power is therefore transferred to the signal resulting to higher gain. An increase in the fibre length means more pump to signal interaction time, which leads to more pump to signal energy transfer, therefore improving the obtained Raman gain. On-off gain is measured to confirm optimum signal-pump wavelength separation for maximum gain. This is used to tune VCSEL to an optimum wavelength corresponding to maximum Raman gain.

4.5. Raman in VCSEL Transmission

The effect of backward pumping scheme and forward pumping scheme on VCSEL data is presented. Figure 4.9 shows BER measurement for data transmission without Raman pumping (black), with backward pumping (red) and forward pumping (blue).
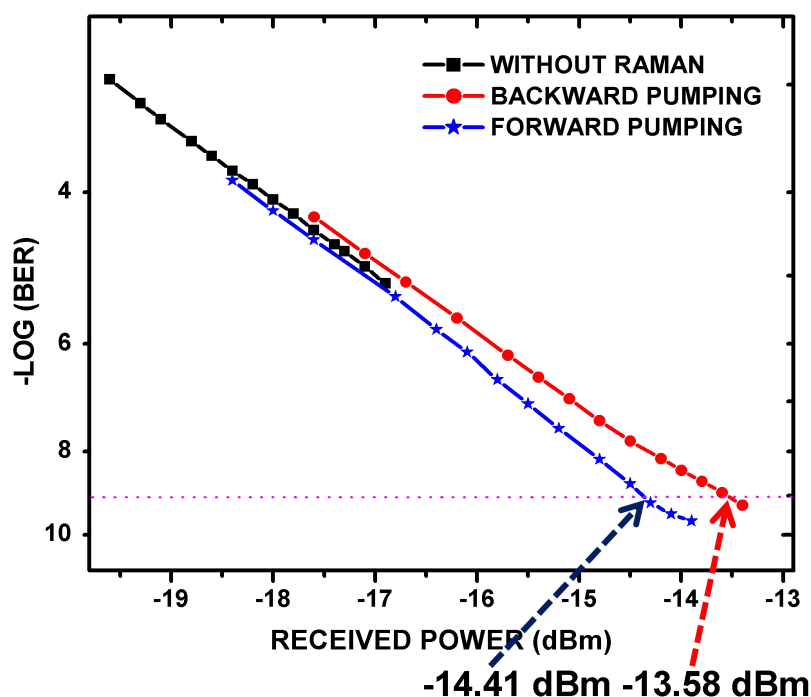
Figure 4.9: Transmission performance for VCSEL Raman assisted technique.

VCSEL without Raman has error flow due to low power and chirping of carrier. Receiver sensitivity for forward pumping and backward pumping was -14.41dBm and -13.58 dBm respectively. Forward pumping has lower receiver sensitivity than backward pumping a property that makes it a better candidate for enhancing VCSEL data. Corresponding eye diagrams for VCSEL without Raman, VCSEL with backward pumping and VCSEL with forward pumping are shown in Figure 4.10 (a), (b) and (c) respectively.
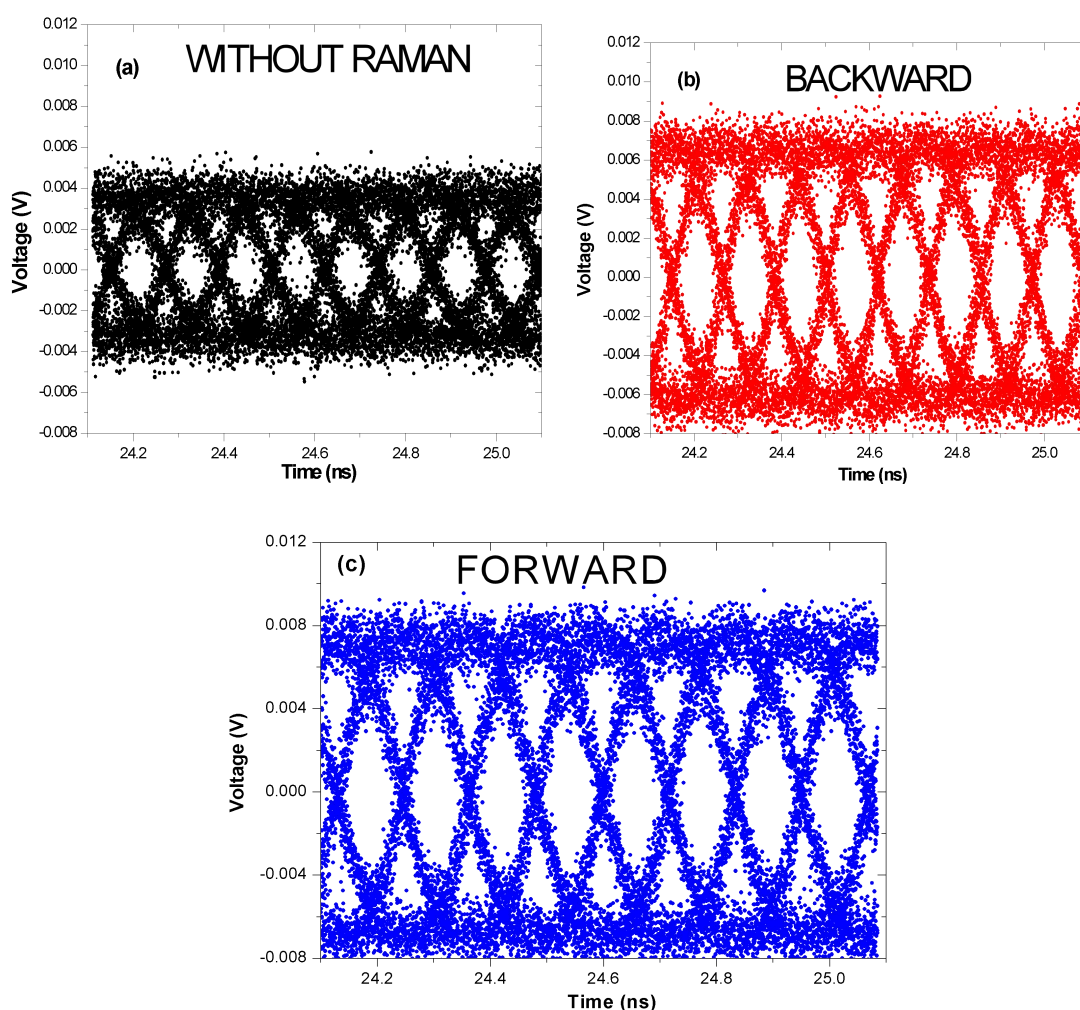
Figure 4.10: Eye diagrams for a fibre length with, (a) No Raman Pump (b) Backward Raman pumping (c) Forward Raman pumping.

The eye diagrams are clearly open indicating successful implementation of Raman amplification in VCSEL technology.

The wave patterns for VCSEL without Raman, VCSEL with backward Raman and VCSEL with forward Raman are shown in Figure 4.11. During transmission, the signal suffers from chirping and dispersion. Forward pumping performs better than backward pumping. As the signal and modulated Raman pump power co-propagate in the fibre, power is transferred from modulated Raman pump to the signal resulting to signal amplification hence higher performance.
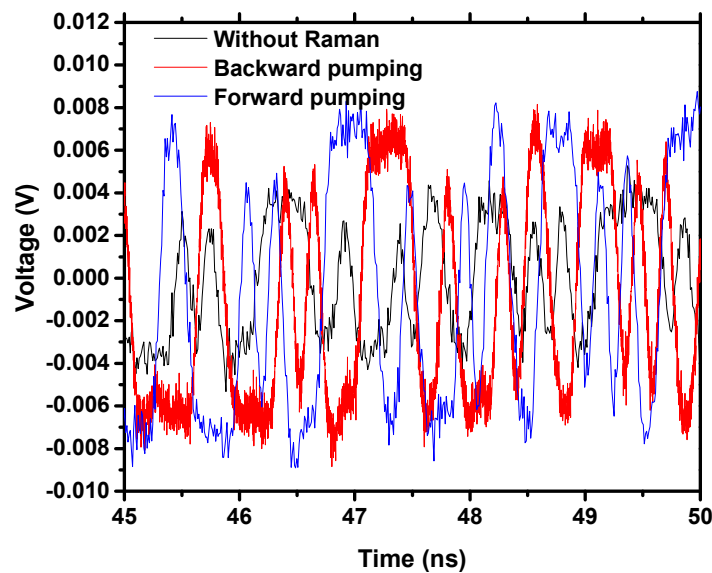
Figure 4.11: Wave patterns for VCSEL signal at the output of a 50.7 km fibre with; no pump (black), backward pumping (red) and forward pumping (blue).

In counter propagation less power is transferred to the signal. The eye for forward pumping has more power than that for backward because of different signal gains. Results on Raman in VCSEL transmission shows that integration of VCSEL and Raman amplification is suited for reach extension and Raman pump reuse in

improving the current transmission systems to meet the future requirement in optical communication systems.

4.6. Demonstration of Integrated extended reach VCSEL interconnect with 8.5 Gbps data modulated forward Raman pump signals

In this section, forward pumping was adopted to demonstrate integrated extended reach VCSEL interconnect. After optimizing for Raman amplification, the transmission performance was evaluated using BER measurements and eye diagram analysis. The Raman pump was used to simultaneously amplify the VCSEL channel as well as to transfer the modulated data over the transmission link, therefore, maximizing the network efficiency. Receiver sensitivities of −14.38, −13.58 and −13.00 dBm were attained for a transmission configuration with un-modulated forward Raman pump, modulated forward Raman pump and modulated backward Raman pump respectively, as shown in Figure 4.12.
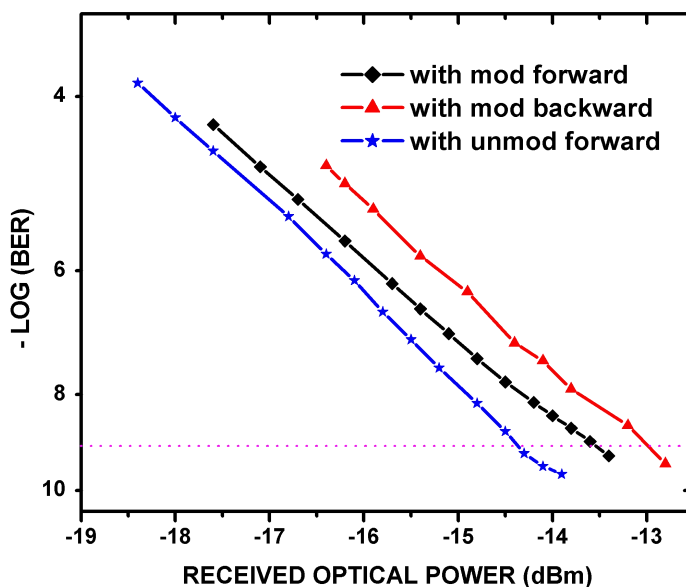
Figure 4.12: BER curves for data transmission with un-modulated forward Raman pump (blue), modulated forward Raman pump (black) and modulated backward Raman pump (red) for link of 50.7 km.

A VCSEL-based Raman assisted transmission link with a modulated forward Raman pump configuration was noted to have a superior performance as opposed to a modulated backward Raman pump configuration. The respective eye diagrams and patterns as collected by a sampling Agilent oscilloscope are shown in Figure 4.13 (a)-(f).
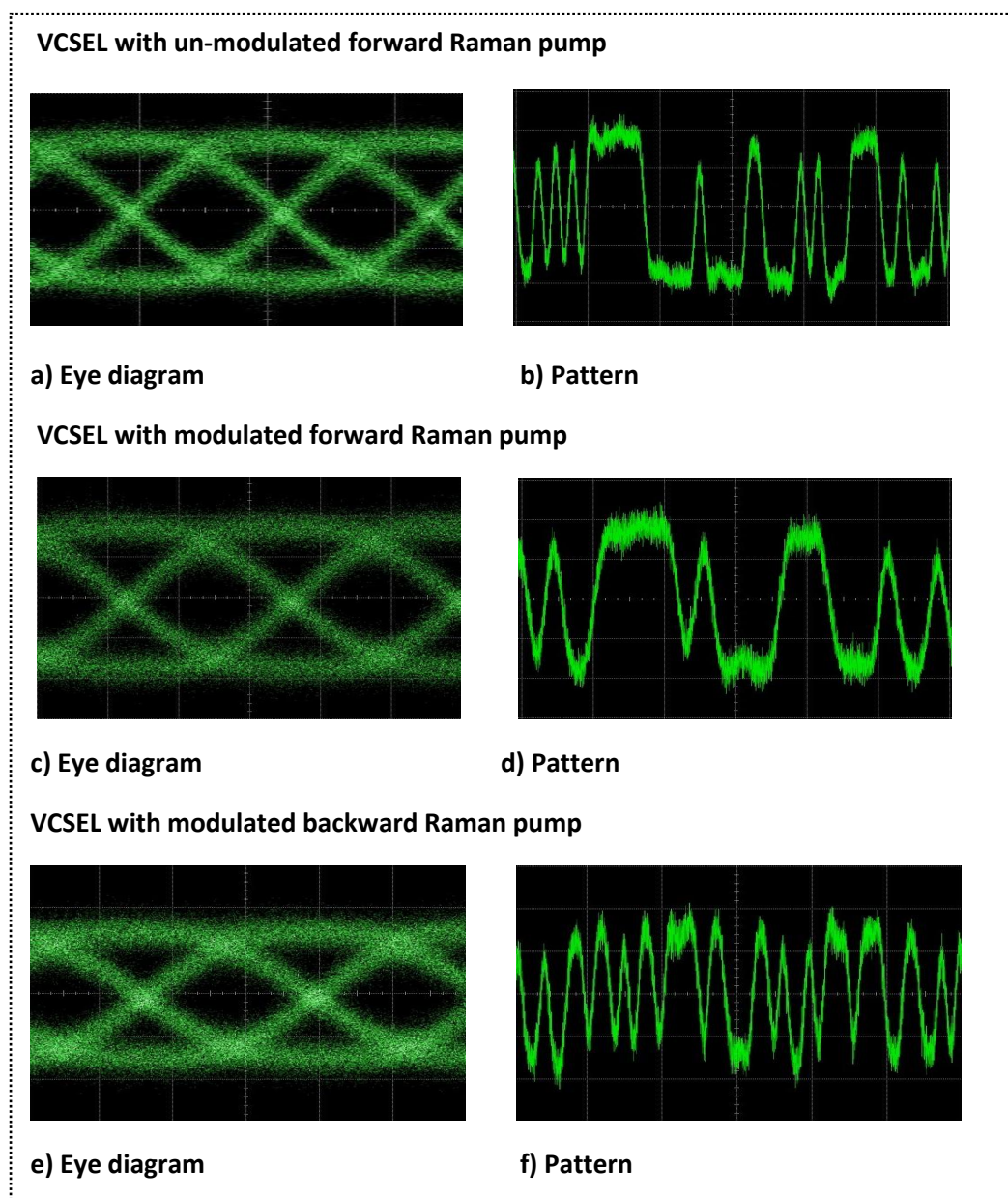
Figure 4.13: Eye diagrams and patterns for (a, b) un-modulated forward Raman, (c, d) modulated forward Raman and (e, f) backward modulated Raman.

The eye diagram results shows that a clearly open eye diagram was achieved in 3 cases scenarios, implying a successful error-free operation. This work, experimentally demonstrated the first reported integrated cross modulated forward pumped DRA with low-cost and power-efficient VCSEL. An 8.5 Gbps modulated forward Raman pump and backward Raman pump suffers a crosstalk penalty of 0.8 dB and 1.38 dB respectively on the transmitted data signal. The compensation from high Raman on-off for forward Raman results in lower power penalty than backward Raman. Overshoot on Raman modulated patterns is chirp arising from high modulation voltage for modulated lasers. This work proves that a key concept for adoption in high capacity wavelength flexible extended reach optical interconnects.

4.7. Raman Assisted-VCSEL for Enhanced Bidirectional Data Transmission

To demonstrate enhanced bidirectional data transmission backward pumping scheme was adopted. To maximize power transfer to the signal, we used strong backward Raman power of 22.01 dBm. VCSEL with un-modulated backward Raman has the wide open and best eye diagram than one for modulated backward and Raman analysis eyes. During transmission the modulated signal is attenuated and interfered with more than un-modulated signal, resulting in eye closure (the more the eye closes, the more difficult to distinguish between 1's and 0's in the signal). Figures 4.14 (a), (c) & (e) shows the open eye diagrams for VCSEL with un-modulated Raman, VCSEL with modulated Raman and Raman pump analysis respectively. The pattern for modulated backward pumping suffers more from chirping compared to un-modulated backward pumping and modulated backward pumping. This is due to cross talk and self interference between the transmitted data.

VCSEL With un-modulated Raman

(a) Eye   **(b) Pattern**

VCSEL with modulated Raman

c) Eye   **(d) Pattern**

Modulated Raman pump analysis

(e) Eye   **(f) Pattern**
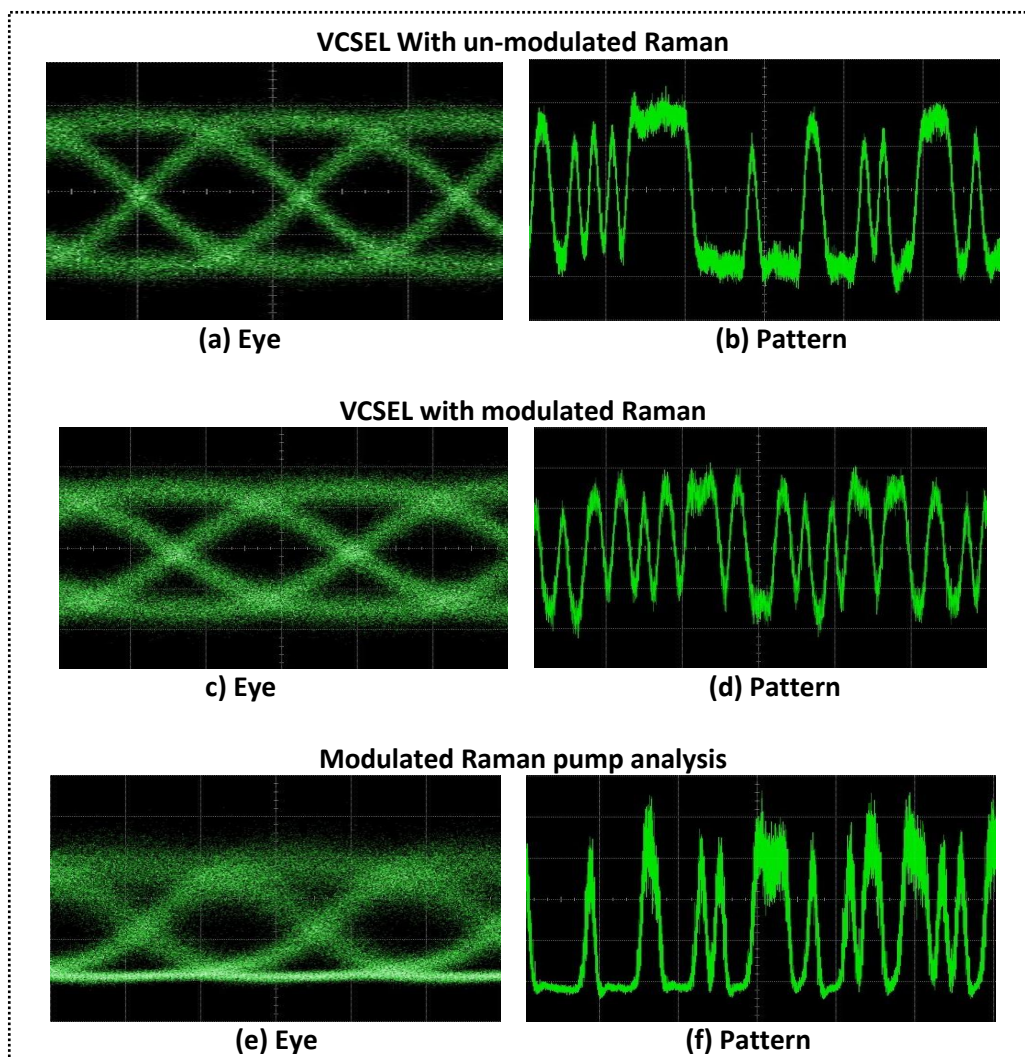
Figure 4.14: Eye diagrams and patterns for (a, b) un-modulated backward Raman, (c, d) modulated backward Raman and (e, f) Raman pump analysis.

While Figure 4.14 (b), (d) & (f) shows the pattern for un-modulated backward pumping, modulated backward pumping and Raman pump analysis respectively. Figure 4.15 shows BER curves for VCSEL with modulated Raman, VCSEL with un modulated Raman and Raman pump analysis. Receiver sensitivities of -14.42 dBm, -14.38 dBm and -13.00 dBm for VCSEL with un-modulated backward Raman, VCSEL with modulated backward Raman and Raman pump analysis respectively was achieved at BER threshold of 10^{-9}.
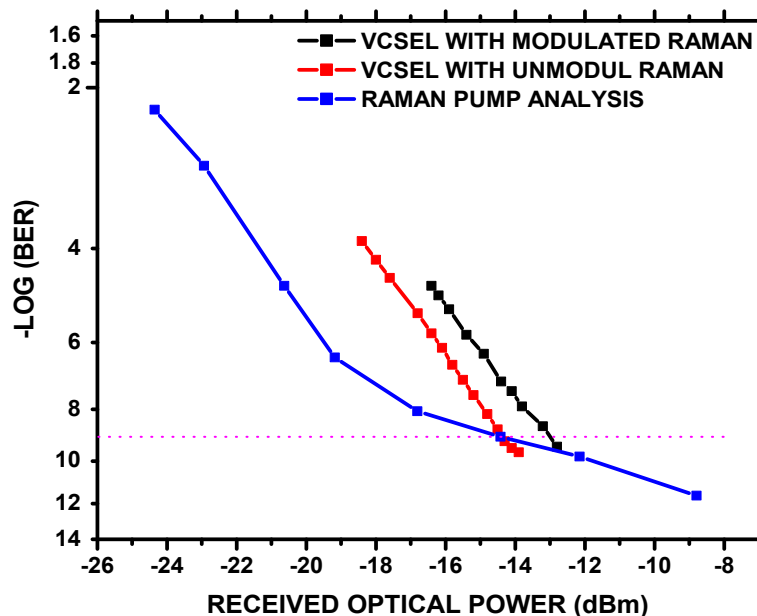
Figure 4.15: BER curves for VCSEL with un-modulated Raman, VCSEL with modulated Raman and Raman pump analysis data transmission

A penalty of 1.42 dB due to self interference on transmitted data was measured. This

work enables integration of VCSEL with Raman pump for enhanced duplex data

transmission and reach extension. In duplex communication, two connected systems

can receive communication simultaneously from both ends. Raman pump was used to

transmit data and enhance VCSEL channel hence attaining bidirectional duplex data

transmission. A duplex bidirectional 8.5 Gbps error-free transmission over 50.7 km

was achieved. This scheme provides a reverse path for the monitoring and remote

adjustment of the equipment in the field. Bidirectional data transmission is key for

networks that send and receive data simultaneously from both ends. Integration of

Raman amplification and VCSEL-based signal transmission is a viable alternative

approach for maximizing reach in next-generation duplex distribution systems.

4.8. Modulated Raman Pump for Integrated VCSEL-based Reach Enhancement and Clock Tone Dissemination in optical Communication

Raman pump was successfully utilized to transmit the clock signal and amplify the transmitted VCSEL data. Clock signals are important in timing applications. Accurate and precise synchronized time and frequency distribution is key to optical communication networks like massive data centers. High speed data transport requires the use of optical fibres to distribute the timing frequency signals as well as data transfer. Figure 4.16 presents the results for backward pumping and forward pumping spectra at 2 GHz, 4 GHz and 6 GHz RF frequency.
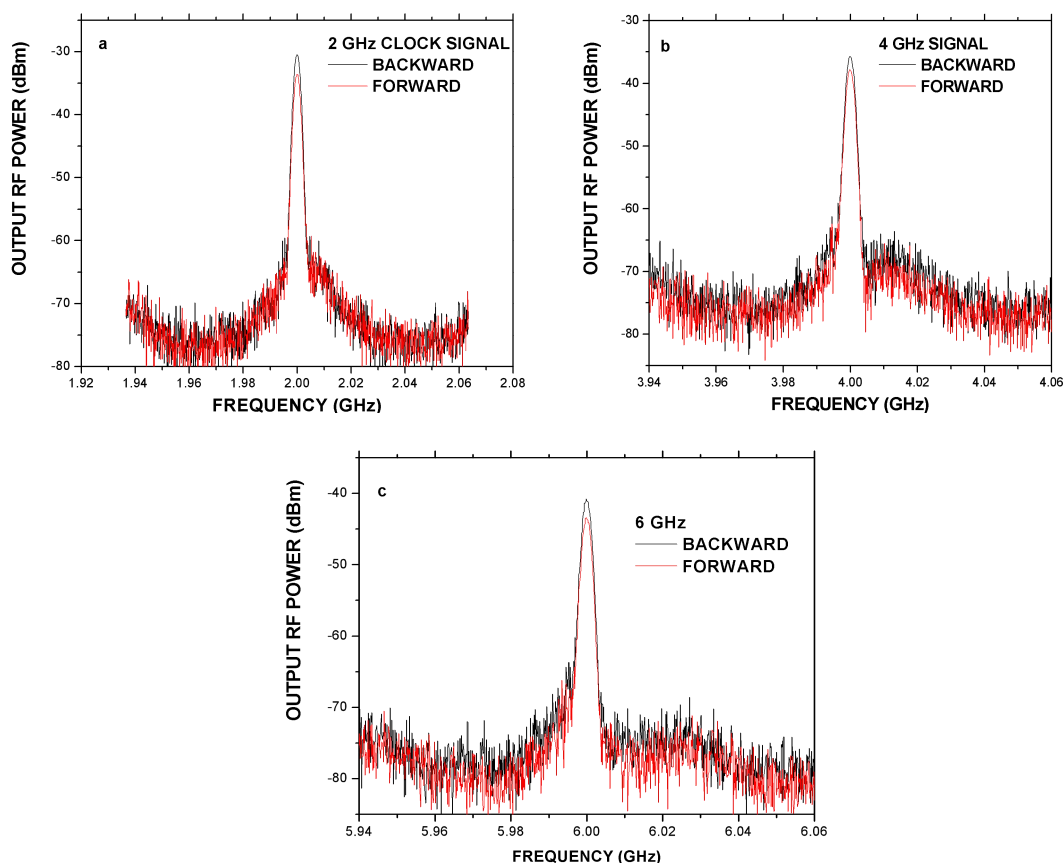

Figure 4.16: Optical spectrums for a) 2 GHz , b) 4 GHz, and c) 6GHz RF frequencies

The peak powers were; -30.67 dBm & -33.83 dBm at 2 GHz; -35.67 dBm & -38.20 dBm at 4 GHz; at 6 GHz -40.67 dBm & -43.62 dBm at 6 GHz for backward and forward pumping respectively. For all the spectra, backward pumping has higher power than forward. As RF clock frequency increases, peak powers reduces because noise sidebands are created on the carrier frequency thus weakening the power in the carrier. The higher the modulation clock frequency the higher the spectrum usage and the low the power. From the Figure 4.17 the phase noise at an offset frequency of 10 kHz for backward pumping at 2 GHz, 4 GHz and 6 GHz was -105.41 dBc/Hz, -109.96 dBc/Hz and -96.49 dBc/Hz respectively, while for forward pumping is -103.04 dBc/Hz, -101.67 dBc/Hz and -96.85 dBc/Hz respectively.
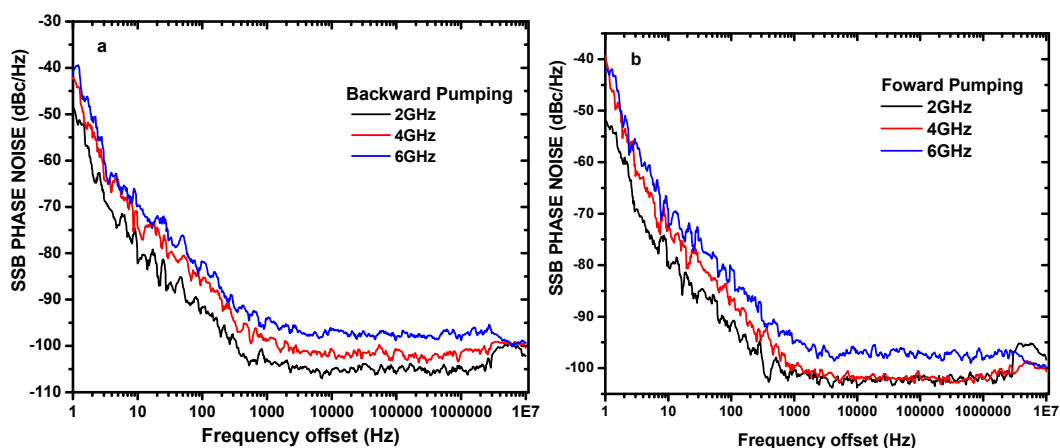
Figure 4.17: **Phase noise evolution as a function of offset frequency at 2 GHz, 4 GHz and 6 GHz RF clock frequency for backward pumping and forward pumping**

Figure 4.18 shows a graph of SSB phase noise against frequency offset as measured using electrical spectrum analyzer (ESA) for electrical signal, forward pumping scheme and backward pumping scheme. The phase noise which is due to frequency variation around nominal central frequency for electrical signal, backward pumped signal and forward pumped signal showed similar noise characteristics. The phase

noise performance for electrical signal, backward and forward signals had a smooth profile with the gradual change of the slope with increasing offset frequency.
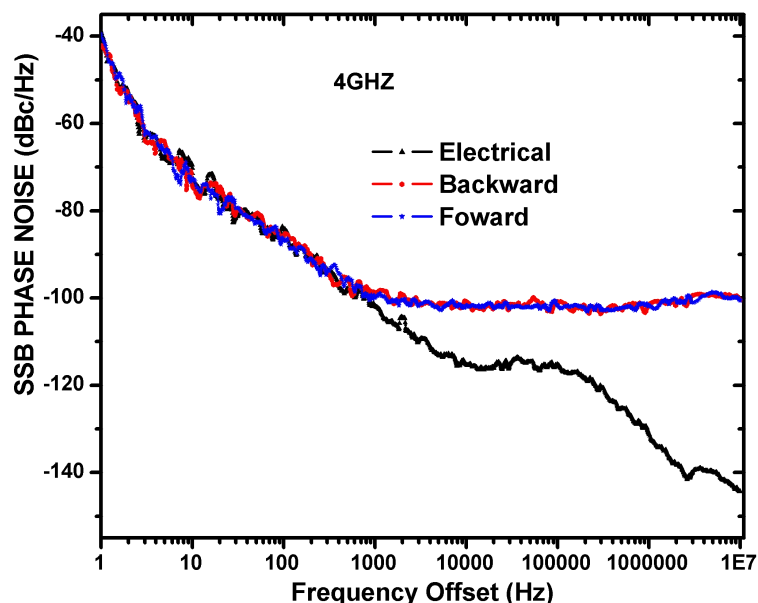
Figure 4.18: SSB phase noise evolution with offset frequency.

The phase noise profile changed with increasing offset frequency. At 10 kHz frequency offset the phase noise obtained was -115.2 dBc/Hz, -100.6 dBc/Hz and -102.2 dBc/Hz for electrical signal, backward and forward signals respectively. As observed in Figure 4.18 phase noise for backward and forward signals were higher than the electrical signal due to the effect of various noise processes in the fibre which degrade the transmitted clock signal by perturbing its phase. Other sources of noise may come from internal reflections at fibre interconnects and polarization mode dispersion (PMD) fluctuations. However, there was an insignificant impact on phase noise for backward and forward signals resulting in a stable transmission of RF clock signal. In this case the data and clock signals were modulated on the intensity of the carrier signal while the clock signal was on the phase of carrier signal, therefore, there was no possibility of interference between the modulated signals as expected. Figure

4.19 shows the experimentally measured spectrum of the 4 GHz RF clock signal over the 50.7 km fibre.
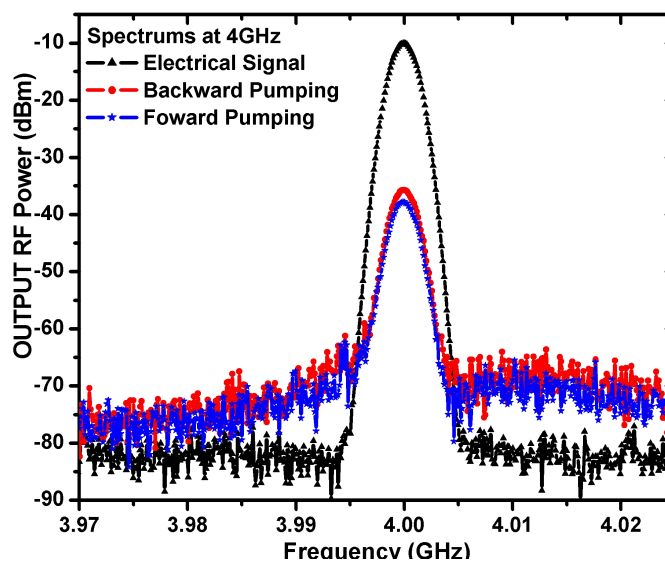
Figure 4.19: Spectra for electrical signal, forward pump and backward pump clock signals

The spectrums have the same characteristic appearance peaking at 4 GHz which was the nominal frequency. The power spectrum analysis plot was used to determine the effect of data transmission at 10 Gbps on the phase noise performance for the 4 GHz clock signal. The forward pumping clock signal had the lowest peak power hence was the most affected by data since it propagates in the same direction in the fibre. The peak powers were -9.8 dBm, -35.4 dBm and -37.9 dBm for electrical signal, backward enhanced signal and forward enhanced signal respectively.

Figure 4.20 shows measured BER curves of the transmission performance for the 1550 nm VCSEL without Raman pump, with forward modulated Raman and un-modulated Raman. VCSEL transmission was analyzed with modulated and un-modulated Raman pump. The receiver sensitivity of -14.12 dBm, -13.7 dBm and -14.8 dBm was obtained experimentally for VCSEL without Raman, VCSEL with un-modulated forward Raman and VCSEL with modulated forward Raman respectively.

Receiver power for modulated Raman was very low and BER curve could not cross the 10^{-9} BER threshold. This is because modulated signal suffers more from the effects of dispersion hence the receiver requires more power to demodulate the signal at the same minimum acceptable BER of 10^{-9}.
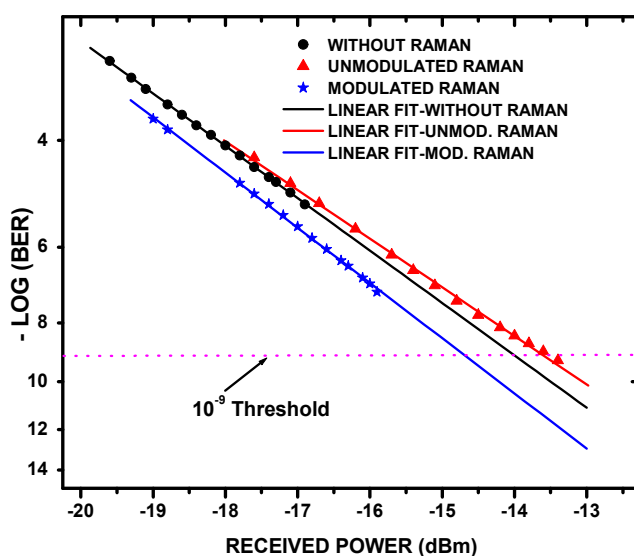
Figure 4.20: Transmission performance for 1550 nm VCSEL Raman assisted technique.

To compensate for accumulated noise in other transmission systems expensive noise cancellation systems which are based on fibre interferometers are used. In this case, accumulated phase noise was minimized by adopting backward pumping to transmit clock signal, which suffers less from phase noise compared to forward.

The eye diagrams for the three scenarios are shown in Figure 4.21. Eye diagram for modulated forward Raman is clearly open compared to the other schemes thus, indicating better performance.
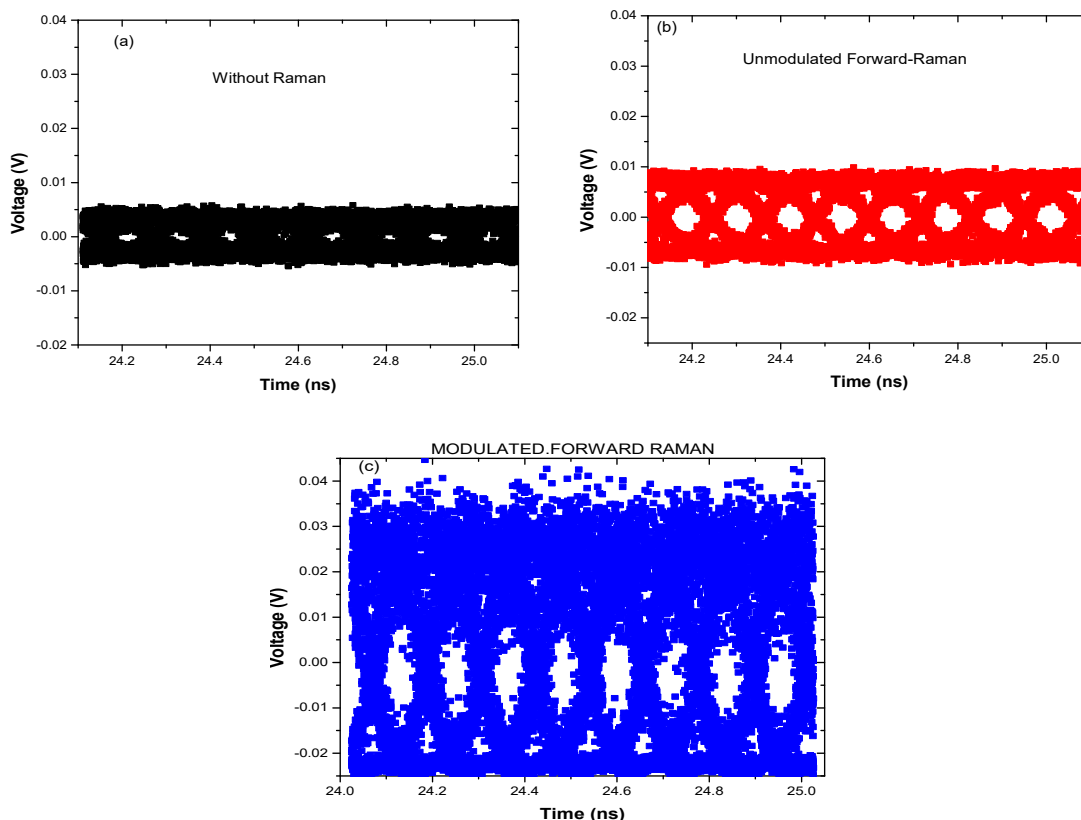
Figure 4.21: Eye diagrams for VCSEL Raman assisted technique (a) VCSEL without Raman, (b) VCSEL with un-modulated Raman and (c) VCSEL with modulated Raman.

The study demonstrates the possibility of real time data transmission enhancement and clock distribution by utilizing VCSEL with Modulated forward Raman. Amplified error-free data transmission and clock signal over long optical fibre with little degradation of frequency stability was realized. Combining VCSEL and modulated Raman is an attractive technique to be adopted in future data centers because forward Raman pump is fully utilized. Since there is no need for an amplifier, this technique is simple and less costly. With Raman assisted VCSEL transmission distance is extended since the signal is amplified. This technique will be of much benefit in LR-PON and data centers.

4.9 RF clock distribution using DFB LASER as a transmitter

4.9.1 Stability of clock signal

Stability results for DFB laser and Raman pump are presented in this section. Before choosing a laser for any optical communication system characterization is important to determine the optimum working for laser. Figure 4.1 shows the optimization results of the considered 1550 nm DFB laser. A 24.69 km optical fibre was used to distribute optical signal and the effect it has on the phase stability of the clock studied. Figure 4.22 (a), (b) and (c) show the results for B2B, DFB and Raman pump at 2 GHz, 4 GHz and 6 GHz RF clock signal.
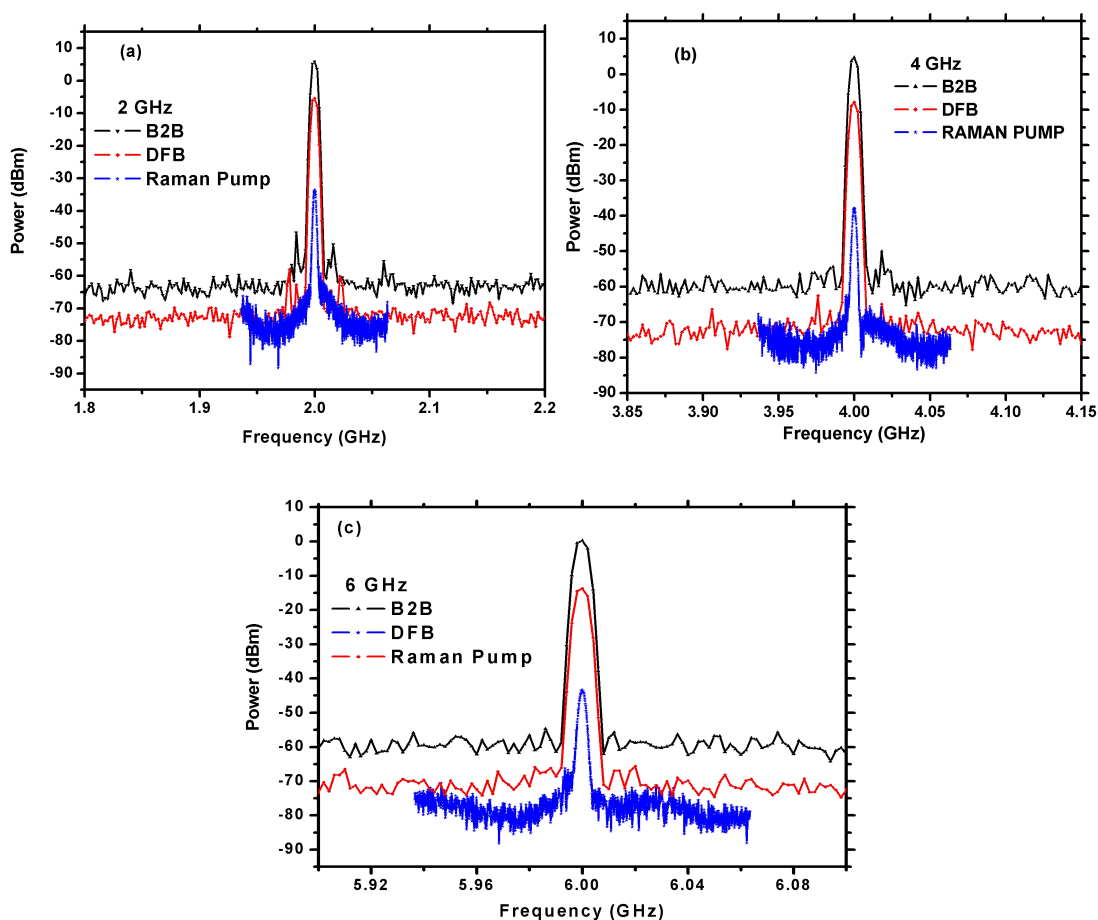

Figure 4.22: Spectra for B2B, DFB laser and Raman pump at (a) 2 GHz clock signal (b) 4 GHz clock signal (c) 6 GHz clock signal.

Peak power for B2B, DFB laser and Raman pump at 2 GHz are; 5.11 dBm, -5.79 dBm and -33.90 dBm respectively; while at 4 GHz we have; 4.74 dBm, -8.34 dBm and -37.58 dBm respectively. Finally peak powers at 6 GHZ for B2B, DFB laser and Raman pump are 0.882 dBm, -13.569 dBm and -42.47 dBm respectively. The results show that spectrum peak power decreases with an increase in RF frequency. B2B peak power for 2 GHz, 4 GHz and 6 GHz RF frequencies are higher than the ones for fibre transmission. This is attributed to fibre impairments. Note that in fibre transfer, mechanical perturbations to the transfer path will influence the fractional instability at a level independent of the carrier frequency. Carrier frequency instability is expressed by averaging carrier frequency and then measuring the power at various offsets from the carrier frequency in a defined bandwidth. It is noted that the peak power for DFB laser for all RF clock frequency is higher than that of Raman pump laser an indication that DFB is suitable for transmitting clock signal over long distance. Carrier frequency for DFB was 1550 nm while that of Raman was 1450 nm and normally at 1550 nm window attenuation in the fibre was minimal. This may have contributed for DFB laser having higher peak power.

Different lasers affect signal central power which in turn affect phase noise. The directly modulated lasers show a higher output than that of the externally modulated source. The weak RF power available means that electronic amplification must be applied to drive the subsequent RF circuitry for phase detection without accumulating a significant amount of additional noise. By measuring the total carrier power and then measuring the noise signal at a specified offset from the carrier, a phase noise measurement can be derived. Phase noise results from frequency variation around the nominal central frequency. As depicted in Figure 4.23 (a) the phase noise at an offset

frequency of 10 kHz for B2B at 2 GHz, 4 GHz and 6 GHz are; -120.27 dBc/Hz, -114.94 dBc/Hz and -111.66 dBc/Hz respectively. While figure 4.23 (b) shows side band phase noise curve for the 24.69 km fibre transmission using the DFB laser and Raman pump. The phase noise for DFB laser at offset frequency of 10 kHz at 2 GHz, 4 GHz and 6 GHz are; -119.93 dBc/Hz, -114.42 dBc/Hz & -111.21 dBc/Hz respectively, while for Raman pump phase noise measured are; -102.50 dBc/Hz, -101.58 dBc/Hz & -96.54 dBc/Hz respectively. Phase noise is observed to increase as RF frequency increases to a higher value. The 24.69 km fibre transmission introduces some instability to the transmitted signal resulting to increase in phase noise. Noise may come from internal reflections at fibre interconnects and polarization mode dispersion (PMD) fluctuations. For all frequencies used, we see similar noise characteristics. Phase noise performance profile changes with increasing offset frequency. As observed in Figure 4.23, 6 GHz RF clock showed the highest phase noise. This is mainly due to noise which degrades the transmitted clock signal by perturbing its phase.
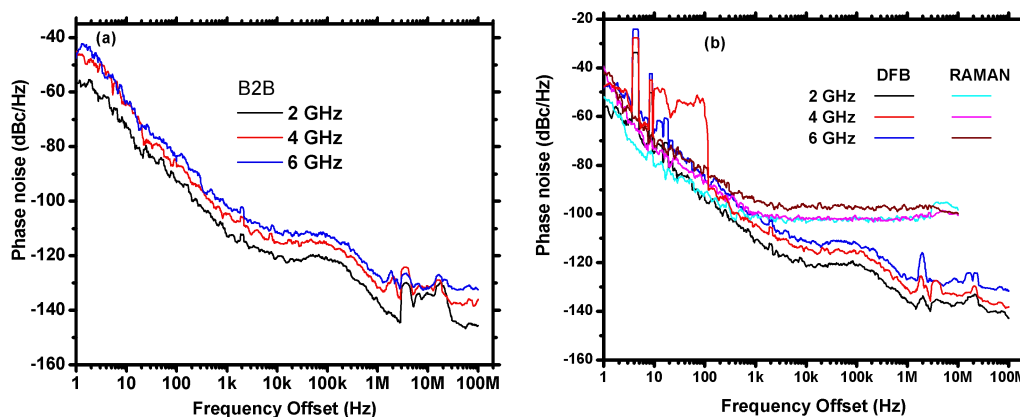

Figure 4.23: (a) SSB phase noise evolution with offset frequency for B2B. (b) Evolution of SSB phase noise with offset frequency at 2 GHz, 4 GHz & 6 GHz for DFB laser and Raman pump.

Different characteristics regions are observed in Figure 4.23. The regions arise from different sources of oscillator noise contribution. Very close to the carrier frequency is predominated with random noise. This noise usually relates to the oscillator physical working environment. If the oscillator is affected by mechanical shocks, vibration, temperature or other environmental effects then random noise will remarkably increase close to the carrier frequency. Flicker noise was seen to dominate between 1 Hz and 10 kHz. Flicker phase noise may be related to physical resonance mechanism of an oscillator, the choice of parts used for the electronics design of the oscillator, but it is usually added by noisy electronics. However, flicker phase noise may be minimized by a quality low noise amplifier design and other electronic components. White phase noise, on the other hand, is a broadband phase noise and has little to do with the resonance mechanism. Different stages of amplification are usually responsible for white noise accumulation. It can be minimized through a high quality amplifier design or by increasing power of primary frequency source to avoid unnecessary amplification. For all RF clock used, phase noise for DFB is lower than Raman pump. However, the phase noise curve for Raman is averagely smooth hence more stable than DFB laser. At offset frequency below 500 Hz DFB clock signal suffered higher phase fluctuations which dramatically degrade the system performance. The difference in performance for the two lasers may be attributed to differences in the structural designs, semiconductor material used and operating specifications. The DFB laser has the highest peak power and best noise performance with the lowest phase noise of -118.65 dBc/Hz at 10 kHz offset frequency. Consequently, using a DFB transmitter for frequency distribution would result in a simple and economical method that will satisfy remote frequency user's demands.

Potential users are laboratories involved in clocks/oscillators development, high-resolution spectroscopy, radio astronomy observations and relativistic geodesy.

4.9.2 Allan Deviation

Allan deviation $\sigma_y (\tau)$ is useful for characterizing a frequency source because the type of phase noise present is revealed by how $\sigma_y (\tau)$ depend on period, τ. Figure 4.24 shows that stability of the device improves as the averaging period gets longer since some noise types can be removed by averaging. At the noise floor, however, more averaging did not improve the results. Allan deviation (long term stability) was demonstrated for 2 GHz and 4 GHz RF frequency using DFB laser as the transmitter. The long term stability measurement of the RF clock signal was analyzed using Allan deviation. Figure 4.24 shows a log-log plot of Allan deviation as a function of averaging time (sigma tau) for B2B and 24.69 km. At 1000 s averaging time Allan deviation obtained for B2B was $1.166 \ e^{-12} /s$.
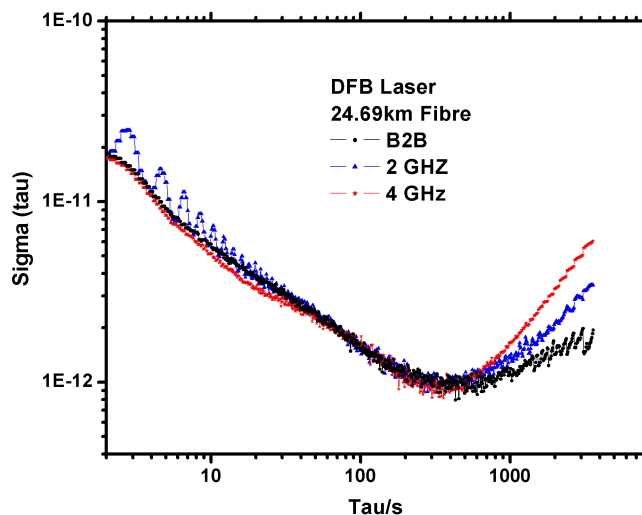

Figure 4.24: The DFB laser clock noise log-log plot of Allan deviation for B2B, and 2 GHz & 4 GHz RF clocks over 24.69 km fibre.

After 24.69 km fibre transmission, Allan deviation of 1.366 e^{-12} /s and 1.626 e^{-12} /s were obtained for 2 GHz and 4 GHz modulation frequency after 1000 s averaging time. The stability curve also showed different slopes implying different noise sources cumulatively contributing to the overall instability of the RF signal. Noise contribution for the first 100 s of averaging time was different from noise contribution after the first 100 s. This is seen with different gradient experienced between the two averaging time regions. In the first 100 s of the resultant spectra band, overlap was noted to reduce with an increase in modulation RF clock frequency. For time scale above 1000 s, the frequency stability is mainly restricted by the electronic components, temperature sensitivity in the phase compensation feedback network. For long averaging the slope decreases which is attributed mainly to temperature fluctuations of the small residual uncompensated fibres. Allan deviation is useful in characterizing a frequency source since the type of phase noise present is revealed by how it depends on the period. These results shows that it is possible to transfer stable and accurate optical frequency over long distances in optical fibre.

CHAPTER FIVE

CONCLUSIONS AND RECOMMENDATIONS

5.1 Conclusions

In this thesis, results for characterization of VCSEL and DFB lasers, Raman amplification and VCSEL in data transmission were presented. Furthermore, Raman amplification in VCSEL data transmission over extended reach, Raman pump reuse for spectral efficient networks and the distribution of timing signals were investigated. Finally, characterization of RF clock signal stability on modulated Raman pump wavelength and the distribution of RF clock using DFB laser and Raman pump were evaluated. The results indicate that Raman gain increases with an increase in pump power for both pumping schemes. Forward pumping scheme performed better than backward pumping for the fibres used with a maximum gain of 6.5 dB for 50.48 km. Forward pumping showed relatively low receiver sensitivity than backward pumping making forward pumping a better candidate for enhancing transmitted data. The eye diagrams for both schemes were clearly open indicating successful enhanced data transmission.

Using a directly modulated 1550 nm VCSEL laser to counter-propagate with modulated backward Raman pump error free data transmission with minimum receiver sensitivity of -14.42 dBm for signal analysis with modulated backward Raman at BER threshold of 10^{-9} was realized. Modulated forward Raman pump was used to maximize network efficiency by simultaneously amplifying VCSEL channel and transmitting data over unidirectional transmission link with minimum receiver sensitivity of -14.38 dBm for un-modulated forward Raman pump.

Simultaneous data and clock distribution technique was realized by exploiting forward and backward Raman pumping over 50.7 km fibre. We modulated VCSEL with 10 Gbps data and coupled into a 50.7 km fibre using Raman coupler to propagate with 4 GHz modulated Raman pump. Amplified error-free data with a minimum receiver sensitivity of -14.8 dBm for modulated forward Raman was achieved. Stable clock dissemination with maximum phase noise of -100.6 dBc/Hz at 10 kHz offset frequency over 50.7 km True Wave Reach fibre was experimentally realized.

Performance characterization of DFB laser on transmitted RF clock signals was analyzed. Minimum phase noise of -119.93 dBc/Hz at 10 kHz offset frequency and Allan deviation of 1.63 e^{-12} /s was obtained for 24.69 km fibre respectively at 100 s averaging time for the 2 GHz clock signal. Proper choice of lasers and modulation levels enhances stability for time and frequency reference systems. DFB laser and Raman pump were successfully utilized to transmit clock signals which are important in timing applications. Raman pump compatibility with VCSEL and reuse capability makes it the best candidate for integrated optical transmission links. However, DFB laser is suited for transmitting the clock signal only and would promotes high stability of the optical carrier.

A novel scheme of simultaneously enhanced bidirectional and unidirectional data/clock transmission was achieved. A real-time technique for transmitting accurate data and stable clock signal for long-reach optical networks employing both backward and forward Raman pumping with power efficient VCSELs for simultaneous data amplification and transmission. Data and clock transmission over 50.7km was successfully demonstrated using a Raman pump for backward and forward pumping schemes. Combining VCSEL and modulated Raman is an attractive technique to be

adopted in future data centers because the Raman pump is fully utilized. Since there is no need for an amplifier, our techniques are simple and less costly. Configuration flexibility, compatibility with widely accepted standards and transparency for transmitted data makes our techniques attractive for commercial optical network operators. This work offers enabling techniques for simultaneous network capacity, efficiency and reach optimization for next-generation optical interconnects.

5.2 Recommendations

This research strongly recommends the use of VCSEL light source and Raman amplification for application in integrated optical transmission links. Use of modulated Raman pump with VCSEL technology for enhanced data and clock transmission in upgrading next generation transport system like radio astronomy is highly recommended. Adoption of enhanced unidirectional and bidirectional data transmission in hyper-scale data centers for long-haul transmission is highly tenable. DFB laser to be used on a system that only transmit clock signals. Raman pump used in enhancing VCSEL data at the same time reused to transmit clock signals. Future work should be done on implementing Raman amplification in extending reach for 5G carrier signals and modulate Raman pump with PAM3 and PAM 4 for high capacity data transmission. Research to be done on generating 5G signals using Raman pumps.

REFERENCES

Agrawal G. (2001). *Nonlinear Fiber Optics.* San Diego, USA: Academic Press.

Agrawal G. P. (2002). *Fiber-Optic communication system.* The Institute of optics University of Rochester.

Agrawal G., Lin Q.,. (2003). Statistics of polarization-dependent gain in fiberbased Raman amplifiers. *Optics Letters , 28* (4), 227–229.

Agrawal G.P. (2005). *Lightwave Technology: Telecommunication Systems.* Wiley, Hoboken.

Agrawal G. P. (2006). *Nonlinear Fiber Optics.* Academic Press.

Agrawal, G. P. (2007). *Nonlinear Fibre Optics 4th edition* (4th ed.). San Diego: Academics Press.

Alexander K., Ahmed A., Dietmar W., and Rainer M. (2013). Monolithic VCSEL–PIN Photodiode Integration for Bidirectional Optical Data Transmission. *IEEE Journal of Selected Topics in Quantum Electronics , 19* (4), 6100313.

Azizoglu P. A., Humblet M. (1991). On the bit error rate of lightwave systems with optical amplifiers. *Journal of Lightwave Technology , 9* (11), 1576-1582.

Bai Y., Wang B., Zhu X.,. (2013). Fiber-based multiple-access optical frequency dissemination. *Optics letters , 38* (17), 3333-3335.

Barnes J. A. (1971). Characterization of frequency stability. *IEEE Transactions on Instrumentation and Measurement , 20* (2), 105-120.

Basu P. K. "Silicon photonics: silicon Raman lasers," *Resonance* 12,37–46 (2007)

Bondurant W. A., Atia R. S. (1999). Demonstration of return-to-zero signaling in both OOK and DPSK formats to improve receiver sensitivity in an optically preamplified receiver. *1999 IEEE LEOS annual meeting conference proceedings.*

Calhoun M., Huang S., and Tjlelker R. L. (2007). Stable photonic links for frequency and time transfer in the deep space network and antenna arrays. *In the Proceedings of IEEE, 95*, pp. 1931–1946.

Cartledge J. C., Burley G. S.,. (1989). The Effect of Laser Chirping on Lightwave System Performance. *Journal of Lightwave Technology , 7* (3), 568–573.

Chinlon L., Rogers H. S. (1976). Backward Raman amplification and pulse steepening in silica fibers. *Applied Physics Letters , 29* (7), 428.

Claps R., Raghunathan V., Dimitropoulos D., and Jalali B. (2004). Influence of nonlinear absorption on Raman amplification in Silicon waveguides. *Optics Express , 12* (12), 2774-2780.

Clifford H., and Agrawal G. P.,. (2005). *Raman Amplification in Fibre Optical Communication Systems.* Elsevier Academic Press, USA.

Company, F. (2013). Retrieved January 27, 2017, from http://www.myvcsel.com/designingwith-vcsels/

Dahiya P., Himanshi S., Amit K.,. (2014). Impact of Hybrid Optical Amplifiers in High Speed Networks. *International Journal of Wireless Communications and Networking Technologies , 3* (3), 44-48.

Dakin J. P., Pratt D. J. (1985). Distributed optical fibre raman temperature sensor using a semiconductor light source and detector. *Electronics Letters , 21* (13), 569-570.

Davey, R. (2006). DWDM Reach Extension of a GPON to 135 km. *Journal of Lightwave Technology , 24* (1), 29-31.

Dhoore S., Köninger A., Meyer R., Roelkens G., and Morthier G. (2019). Electronically tunable distributed feedback (DFB) laser on silicon. *Laser & Photonics Reviews , 13* (3), 1-7.

Dolfi, D. (2003). Multi-channel optical interconnects for short-reach applications. *Proceedings of the 53rd Electronic Components and Technology Conference*, (pp. 1032–1039). New Orleans, LA, USA .

Drögemüller K., Kuhl D., Blank J., Ehlert M., Kracker T., Höhn J., Klix D., Plickert V., Melchior L., Schmale I., Hildebrandt P., Heinemann M., Schiefelbein F. P., Leininger L., Wolf H. D., Wipiejewski T., Ebberg A. (2000). Current progress of advanced high speed parallel optical links for computer clusters and switching systems. *Proceedings of the 50th Electronic Components and Technology Conference*, (pp. 1227-1235). Las Vegas, NV, USA,.

Emilie R., Christophe M., Lionel R., Jean-Luc I., Michel B.,. (2006). Phase noise in GNSS transmission / reception system. *National Technical Meeting of The Institute of Navigation*, (pp. 698-708). Monterey, United State.

Foreman S. M., Holman K. W., Hudson D. D., Jones D. J., and Ye J. (2007). Remote transfer of ultrastable frequency references via fibre networks. *Review of Scientific Instruments , 78*, 021101.

Fugihara M. C., Pinto A. N. (2008). Low-Cost Raman Amplifier for CWDM Systems. *Microwave and Optical Technology Letters , 50* (2), 297-301.

Fujieda M, Kumagai M, Nagano S,. (2011). All-optical link for direct comparison of distant optical clocks. *Optics express , 19* (17), 16498-16507.

Gibbon T B, Prince K, Neumeyr C, Rönneberg E, Ortsiefer M. (2010). 10 Gb/s 1550 nm VCSEL transmission over 23.6 km single mode fibre with no dispersion compensation and no injection locking for WDM PONs. *Proceeding of Optical Fibre Communication & the National Fibre Optics Engineering Conference.* San Diego, CA, USA.

Grosche G., Terra O., Predehl K., Holzwarth R., Lipphardt B., Vogt F., Sterr U., and Schnatz H. (2009). Optical frequency transfer via 146 km fiber link with 10^{-19} relative accuracy. *Optics Letters , 34* (15), 2270-2272.

Hahn K., G. K. (1999). *VCSEL-based fibre-optic data communication, in Vertical Cavity Surface Emitting Lasers.* Cambridge: Cambridge University Press.

Hofmann W., Gruner-Nielsen L., Ronneberg E., Bohm G., Ortsiefer M., Amann M. (2009). 1.55-μm VCSEL modulation performance with dispersion-compensating fibres. *IEEE Photonic Technology Letters , 21* (15), 1072–1074.

Hofmann W., Müller M., Wolf P., Mutig A., Gründl T., Böhm G., Bimberg D., and M.-C. Amann M. C. (2011). 40 Gbit/s modulation of 1550 nm VCSEL. *Electronic Letters , 47* (4), 270–271.

Holman K. W., Jones D. J., Hudson D. D., Ye J.,. (2004). Precise frequency transfer through a fibre network using 1.5-μm mode-locked sources. *Optics Letters , 29* (13), 1554- 1556.

Honjo T., Inoue T., and Inoue K. (2011). Influence of light source linewidth in differential- phase-shiftquantum key distribution systems. *Optics Communication , 284*, 5856– 5859.

Hossain M. S., Howlader S., Basak R.,. (2015). Investigating the Q-factor and BER of WDM system in optical fibre Communication Network using SOA. *International Journal of innovation and scientific research , 13* (1), 315-322.

Huan S., Byoung W. K., and Biswanath M. (2010). Long-Reach Optical Access Networks: A Survey of Research Challenges, Demonstrations, and Bandwidth Assignment Mechanisms. *IEEE Communications Surveys & Tutorials , 12* (1), 112-123.

Iga, K., Laboratory Notebook, (March 22 1977)

Iga, K. (2000). Surface-emitting laser-its birth and generation of new optoelectronics field. *IEEE Journal of Selected Topics in Quantum Electronics , 6* (6), 1201–1215.

Islam M. (2004). *Raman Amplifiers for Telecommunications 2: Sub-systems and Systems.* New York: Springer-Verlag.

Islam, M. N. (2003). *Raman Amplifiers for Telecommunications I.* Springer.

Isoe G. M., Kiboi Boiyo D., Rotich E. K., Osiemo D. M., Gibbon T. M. (2019). Integrated extended reach VCSEL interconnect with 8.5 Gbps data modulated forward Raman pump signals. *Journal of Modern Optics , 66* (19), 1913-1919.

Isoe G.M; Wassin S.; Leitch A.W.R.; Gibbon T.B.,. (2018). 60 Gbps 4-PAM VCSEL-based Raman assisted hyper-scale data centre: In context of spectral efficiency and reach extension. *Optics communication , 428*, 164-168.

Isoe G. M., Muguro K. M., and Waswa D. W. (2013). Noise Figure Analysis of Distributed Fibre Raman Amplifier. *International journal of scientific & technology research , 2* (11), 375-378.

Isoe G.M., Muguro K., Waswa D., Osiemo D.M., Kirui E., Cherutoi H.,. (2014). Forward Raman Amplification Characterization in Optical Networks. *Proceedings of 2014 international conference on Sustainable Research and Innovation. 5*, pp. 251-253. JKUAT.

Jespersen J. (1970). Survey of Time and Frequency Dissemination Techniques . *24th Annual Symposium on Frequency Control.*

Kaminov I. P. (1981). Polarization in Optical Fibers. *IEEE Journal of Quantum Electronics .*

Katsuyama T. (2009). Development of semiconductor laser for optical communication. *SEI Technical Review , 69*, 13-20.

Kefelian F., Lopez O., Jiang H., Chardonnet C., Amy-Klein A., and Santarelli G. (2009). High resolution optical frequency dissemination on a telecommunications network with data traffic. *Optics Letters , 34* (10), 1573–1575.

Keiser G. (2011). *Optical fibre communication .* New York: McGraw-Hill.

Kiboi B., Gibbon T. B., Rotich Kipnoo E. K. (2018). A VCSEL-based backbone extended-reach optical fibre network: Supporting up to 10 Gbps flexible access networks for Africa. *Journal Optical Fibre Technology , 43*, 126-130.

Koonen, T. (2005). Fibre-optic techniques for broadband access networks. *Telektronikk , 101* (2), 49–65.

Krehlik et al. (2016). Fibre Optic Time and Frequency Distribution Technology — A General Characterization and Fundamental Limits. *IEEE Transanctions Ultrasonics, Ferroelectrics, and Frequency Control , 63* (7), 993–1004.

Krehlik P., Śliwczyński Ł., Buczek Ł.,. (2015). Ultrastable long-distance fibre-optic time transfer: active compensation over a wide range of delays. *Metrologia , 52* (1), 82.

Laming R.I., Morkel P.R., Payne D.N., Reekie L,. (1988). Noise in Erbium-Doped Fibre Amplifers. *Fourteenth European Conference on Optical Communication*, *1*, pp. 54–57.

Larsson A., Simpanen E., Gustavsson J. (2018). 1060nm VCSELs for long-reach optical interconnects. *Optical Fibre Technology , 44*, 36-42.

Lau K. Y., George F. L., and Robert L. T. (2014). Ultra-stable RF-over-fibre transport in NASA antennas, phased arrays and radars. *Journal of Lightwave Technology , 32* (20), 3440–3451.

Levi, A. (2000). Optical interconnects in systems. *Proceedings of the IEEE June 2000*, *88 (6)*, pp. 750–757.

Lewandowski W., Azoubib J., Klepczynski W. J. (1999). GPS: Primary tool for time transfer. *Proceedings of the IEEE*, *87(1)*, pp. 163-172.

Li W., Zhang X., and Yao J. (2013). Experimental demonstration of a multiwavelength distributed feedback semiconductor laser array with an equivalent chirped grating profile based on the equivalent chirp technology. *Optics Express , 21*, 19966-19971.

Liu X., Xu C., and Wei X. (2002). Nonlinear phase noise in pulse-overlapped transmission based on return-to-zero differential-phase-shift-keying. *European Conference on Optical Communication.*

Logan R. T., Lutes G. F. (1992). High stability microwave fibre optic systems: demonstrations and applications. *Proceedings of the 43rd IEEE annual frequency control symbosium*, (pp. 310-316). Hershey, PA, USA.

Lopez O., Amy-Klein A., DaussyC., Chardonnet Ch., Narbonneau F., Lours M., and Santarelli G. (2008). 86-km optical link with a resolution of 2×10^{-18} for RF frequency transfer. *European Physical journal D , 48* (1), 35-41.

Lopez O., Haboucha A., Kefelian F., Jiang H., Chanteau B., Roncin V., Chardonnet C., Amy- Klein A., and Santarelli G.,. (2010). Cascaded multiplexed optical link on a telecommunication network for frequency dissemination. *Optics Express , 18* (16), 16849–16857.

Lopez O., Haboucha A., Chanteau B., Chardonnet C., Amy-Klei A. N., Santarelli G. (2012). Utra-stable long distance optical frequency distribution using the Internet fibre network. *Optics Express , 20* (21), 23518–23526.

Lopez O., Kanj A., Pottie P. E.,. (2013). Simultaneous remote transfer of accurate timing and optical frequency over a public network. *Applied Physics B , 110*, 3-6.

Lyle C. J., Anderson J. A. (1994). Technique for evaluating system performance using Q in numerical simulations exhibiting intersymbol interference. *Electronics Letters , 30* (1), 71-72.

Marra G., Margolis H. S., Richardson D. J.,. (2012). Dissemination of an optical frequency comb over fibre with 3×10^{-18} fractional accuracy. *Optics Express , 20* (2), 1775- 1782.

Nan D., Zhangweiyi L., Xiaocheng W. (2018). Distribution of a phase-stabilized 100.02 GHz millimeter-wave signal over a 160 km optical fibre with 4.1×10^{-17} instability. *Optics Express , 26* (18), 1339-1346.

Narbonneau F., Lours M., Bize S., Clairon A., Santarelli G., Lopez O., Daussy C.,. (2006). High resolution frequency standard dissemination via optical fibre metropolitan network. *Review of Scentific Instruments , 77* (6), 064701-064708.

Pape A., Terra O., Friebe J., Riedmann M., Wubbena T., Rasel E. M., Predehl K., Legero T., Lipphardt B., Schnatz H., and Grosche G.,. (2010). Long-distance remote comparison of ultrastable optical frequencies with 10^{-15} instability in fractions of a second. *Optics Express , 18* (20), 21477-21483.

Parakhan M. J. (2009). Characteristic of Discrete Raman Amplifier at Different Pump Configuration. *World Academic Of Science Engineering & Technology* , 54.

Peens-Hough A. (2012). *MeerKAT system preliminary design memo series TM Revision 1A, internal report.*

Pelouch, W. (2016). Raman Amplification: An Enabling Technology for Long-Haul Coherent Transmission Systems. *Journal of Lightwave Technology , 34* (1), 6–19.

Petit G., Jiang Z.,. (2008). GPS all in view time transfer for TAI computation. (G. a. computation, Ed.) *Metrologia , 45* (1), 35–45.

Piester D., Bauch A., Breakiron L., Matsakis D., Blanzano B., Koudelka O.,. (2008). Time transfer with nanosecond accuracy for the realization of international atomic time. *Metrologia , 45*, 185-198.

Pozar D. (2001). *Microwave and RF design of wireless systems.* New York, USA: John Wiley & Sons, Inc.

Predehl K., Grosche G., Raupach S. M. F., Droste S., Terra O., Alnis J., Legero T., Hänsch T. W. (2012). A 920-kilometer optical fibre link for frequency metrology at the 19th decimal place. *Science , 336* (6080), 441–444.

Primas L., Lutes G., Sydnor R. (1988). Fibre optic frequency transfer link. *Proceedings of the 42nd Annual frequency control Symposium*, (pp. 478-484).

Prince K., Ma M., Gibbon T. M., and Monroy I. (2010). Demonstration of 10.7- Gb/s transmission in 50-km PON with uncooled free-running 1550-nm VCSEL. *Laser Electro-Optics/Quantum Electronics Laser Science Conference*, (pp. 1-2). San Jose, CA, USA.

Prince, K., Ma, M., Gibbon, T. B., Neumeyr, C., Rönneberg, E., Ortsiefer, M.,. (2011). FreeRunning 1550 nm VCSEL for 10.7 Gb/s Transmission in 99.7 km PON. *Journal of Optical Communications , 3* (5), 399-403.

Raman, C. (1928). A new radiation. *Indian Journal of Physics , 2*, 387-398.

Rodes R. (2012). 100 Gb/s signal VCSEL data transmission link. *Optical Fibre Communication Fibre Optic Engineers Conference*, *10.* Los Angeles, USA.

Rodes R., Pham T. T., Jensen J. B., Gibbon T. B., and Tafur I. M. (2010). Energy-efficient VCSEL-based multi Gigabit IR-UWB over fibre with airlink transmission system. *23rd Annual Meeting of the IEEE Photonics Society*, (pp. 222-223). Denver, CO.

Rong H., Jone R., Liu A., Cohen O., Hak D., Fang A., and Paniccia M. (2005). A continuous- wave Raman silicon laser. *Nature , 433*, 725-728.

Rotich E. K., Gamatham R. G., Leitch A. W. R. and Gibbon T. B. (2017). Simultaneous Signal Amplification and Clock Distribution Employing Backward Raman Pump Over an Optical Fibre for Applications Such as Square Kilometer Array. *Journal of Astronomy and Instrumentation , 6* (3), 17500051-17500056.

Rutman J., Walls F. L. (1991). Characterization of Frequency Stability in Precision Frequency Sources. *Proceedings of the IEEE , 79* (7), 952-960.

Saar B. G., Freudiger C. W., Reichman J., Stanley C. M., Holtom G. R., and Xie X. S. (2010). Video-Rate Molecular Imaging in Vivo with Stimulated Raman Scattering. *Science Translational Medicine , 330* (6009), 1368-1370.

Sato K., Hara T., Kuji S., Asari K., Nishio M.,. (2000). Development of an Ultrastable Fibre Optic Frequency Distribution System Using an Optical Delay Control Module. *IEEE Transactions on Instrumentation and Measurement , 49* (1), 19-24.

Singh S. P., Gangwar R., and Singh N.,. (2007). Nonlinear scattering effects in optical fibres. *Progress in Electromagnetics Research*, *74*, pp. 379–405.

Śliwczyński Ł., Krehlik P., Buczek Ł.,. (2011). Active propagation delay stabilization for optic frequency distribution using controlled electronic delay lines. *IEEE Transactions on Instrumentation and Measurement , 60* (4), 1480-1488.

Śliwczyński Ł., KrehlikP., Czubla A., Buczek Ł, and LipińskiM. (2013). Dissemination of time and RF frequency via a stabilized fibre optic link over a distance of 420 km. *Metrologia , 50* (2), 133–145.

Soda H., Iga K., Kitahara C., and Suematsu Y. (1979). GaInAsP/InP surface emitting injection lasers. *Japanese Journal of Applied Physics* , 2329–2330.

Stefano B. (1997). Clock Stability Characterization and Measurement in Telecommunications. *IEEE Transactions on Instrumentation and Measurement , 46* (6), 1284-1294.

Steger S.T. (2014). *A fundamental approach to phase noise reduction in hybrid Si/III–V lasers.* Ph.D. Thesis, California Institute of Technology.

Stolen R. H., Gordon J. P., Tomlison W. J., and Haus H. A.,. (1989). Raman Response Function of Silica- Core Fibre. *Journal of Optical Society of America B , 6* (6), 1159-1166.

Sullivan, D. B. (1990). Characterization of clocks and oscillators. *National Institute of Standards and Technology* .

Suzuki K. I., Fukada Y., Nesset D., and Davey R. (2007). Amplified gigabit PON systems. *Journal of Optical Networking , 6* (5), 422-433.

Tadokoro T., Kobayashi W., Fujisawa T., Yamanaka T., and Kano F.,. (2011). High-speed modulation lasers for 100GbE applications. *In Optical Fiber Communication Conference/National Fiber Optic Engineers Conference 2011 (OSA/OFC/NFOEC).* Optical Society of America, 2011), paper OWD1.: Optical Society of America, 2011), paper OWD1.

Tatum J. (2015). VCSEL-based interconnects for current and future data centers. *IEEE Journal of Lightwave Technology , 33* (4), 727-732.

Terra O., Grosche G., Predehl K., Holzwarth R., Legero T., Sterr U., Lipphardt B., and Schnatz H. (2009). Phasecoherent comparison of two optical frequency standards over 146 km using a telecommunication fibre link. *Applied Physics B , 97* (541), 541–551.

Trezza J., Iamartino J., Bagheri H., DeCusatis C. (2003). Parallel optical interconnects for enterprise class server clusters: needs and technology solutions. *IEEE Communication Magazine , 41* (2), 36-42.

Olmos J.J., Rodes R., and Tafur I. M.,. (2012). Low power consumption O-band VCSEL sources for upstream channels in PON systems. *Prococeeding of Opto-Electronics and Communications Conference*, (pp. 130-131).

Vig J.R. (2004). Quartz Crystal Resonators and Oscillators for Frequency Control and Timing Applications. *IEEE International Frequency Control Symposium Tutorials.*

Walls F. L. (2001). Laser Frequency Stabilization, Standards, Measurement, and Application. *Proceedings of Society of Photo-Optical Instrumentation Enginerers (SPIE)*, *4269*, pp. 170–177. Bellingham, Washington.

Wang B., Gao C., Chen W. L.,. (2012). Precise and continuous time and frequency synchronization at the 5×10^{-19} accuracy level. *Scientific reports* , 556.

Wasfi M. (2009). Optical Amplifiers Review. *International Journal of Communication Networks and Information Security (IJCNIS) , 1* (1), 42-47.

Williams P A, Swann W C, Newbury N R. (2008). High-stability transfer of an optical frequency over long -optic links. *Journal Optical Society of America B , 25* (8), 1284- 1293.

Windover, L. B. (2005). Parallel-optical interconnects and their applications. *Optical Fibre Communication conference*, *3.* Anaheim, CA, USA.

Witt T. J. (2005). Allan Variances and Spectral Densities for DC Voltage Measurements with Polarity Reversals. *IEEE Transactions on Instrumentation and Measurement , 54* (2), 550-553.

Woodbury E. J., and Nag W. K.,. (1962). First demonstration of stimulated Raman scattering. *IRE Proceedings*, *50*, pp. 2347-2348.

Xueming L. (2004). Optimization for various schemes of distributed fibre Raman amplifiers. *Journal of Optics A: Pure and applied Optics , 6* (11), 1017-1026.

Yan F. L., Taylor R., and Calia D. B. (2009). 150 W highly efficient Raman fiber laser. *Optics Express , 17* (26), 23678-23683.

Yusoff Z., Lee J. H., Belardi W., Monro T. M., Teh P. C., and Richardson D. J. (2002). Raman effects in a highly nonlinear holey fiber: amplification and modulation. *Optics Letters , 27* (6), 424-426.

Zhang S., Zhao J. (2015). Frequency comb-based multiple-access ultrastable frequency dissemination with 7× e^{-17} instability. *Optics letters , 40* (1), 37-40.

Zhang X., Li Z., Li J., Yu C., Lau A. P., and Lu C. (2014). Low-cost coherent receiver for long- reach optical access network using single-ended detection. *Optics Letters , 39* (18), 5248–5250.

APPENDICES

Appendix I

Journal Publications

1. G. M. Isoe, D. Kiboi Boiyo, E. K. Rotich, **D. M. Osiemo** & T. B. Gibbon (2019): Integrated extended reach VCSEL interconnect with 8.5 Gbps data modulated forward Raman pump signals, Journal of Modern Optics

2. **Osiemo, D. M**., Waswa, D. W., Muguro, K. M., Isoe, George, Gibbon, Tim, Leitch, A. W. ' Modulated Raman pump for integrated VCSEL-based reach enhancement and clock tone dissemination in optical communication' Optics Communications (2019)

3. **Osiemo, D. M**., Waswa, D. W., Muguro, K. M., Isoe, George, Gibbon, Tim, Leitch, A. W. 'Frequency stability characterization: DFB laser and Raman pump performance on a distributed clock signal over 24.69 km fiber' Optical Society of America A (2020)

Appendix II

Experimental Components
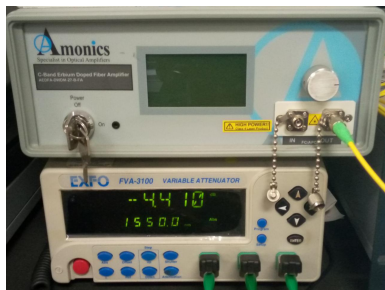
Attenuator

BERT/Signal generator
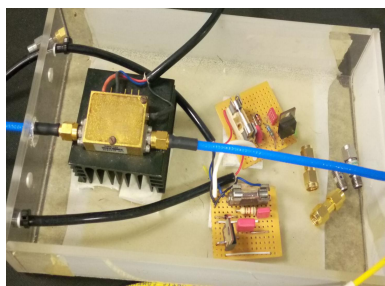
Electrical amplifier

Fan
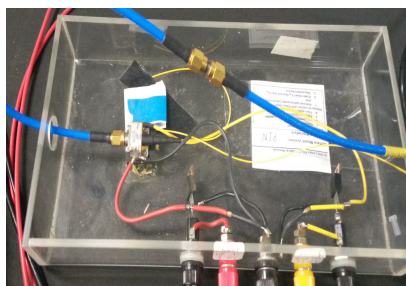
PIN Photodiode

Polarization controller

(Source : Author, 2019)
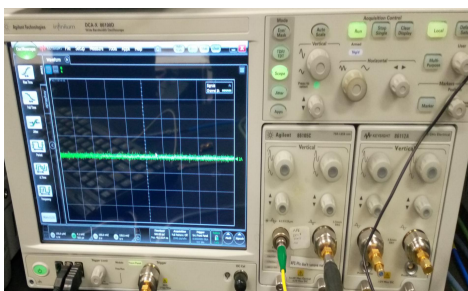
Optical spectrum analyzer
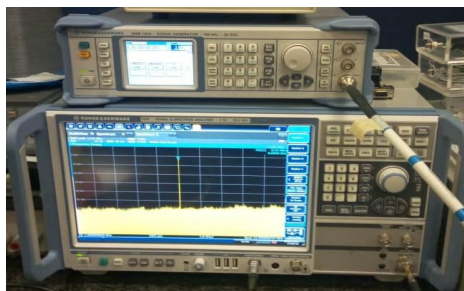
ESA and RF generator

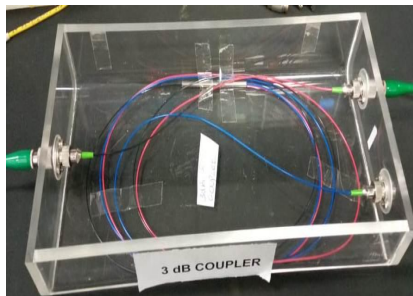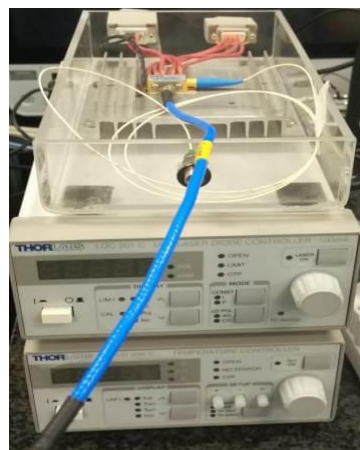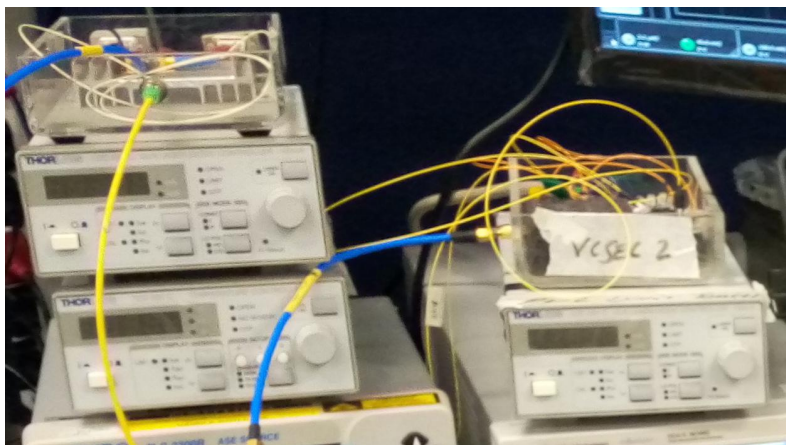Fibre spools

Power meter
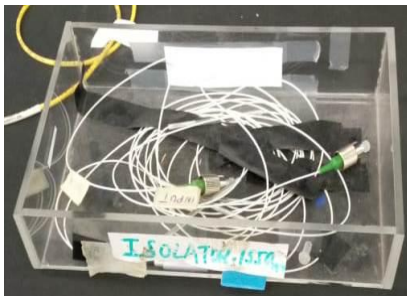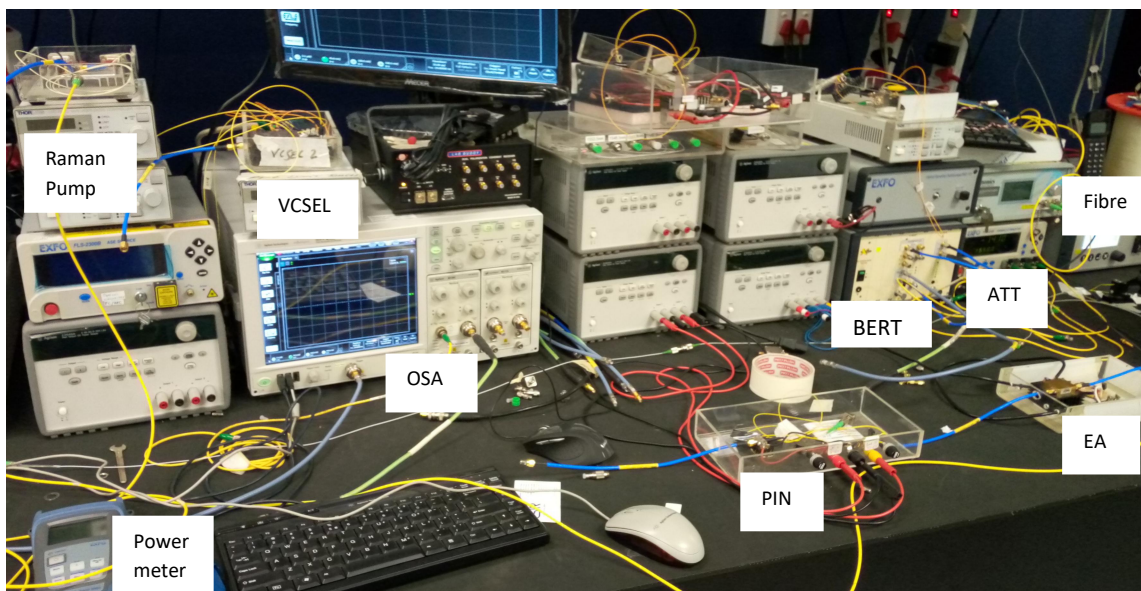

Isolator

Optical coupler

Raman pump

DFB Laser

VCSEL Lasers

Experimental Setup

(Source : Author, 2019)

Appendix III : SIMILARITY REPORT

Document Viewer

Turnitin Originality Report

Processed on: 25-Feb-2022 12:08 EAT
ID: 1642529507
Word Count: 21997
Submitted: 4

SC/PHD/006/16 By Douglas Osiemo

Similarity Index	Similarity by Source	
	Internet Sources:	12%
19%	Publications:	13%
	Student Papers:	4%

include quoted   include bibliography   excluding matches < 4 words   mode:

| quickview (classic) report ⌄ | Change mode | print | refresh | download |

<1% match (Internet from 30-Nov-2018)
http://ijrtm.com

<1% match (Internet from 30-Mar-2010)
http://www.fastbit.com

<1% match (Internet from 15-Jan-2022)
https://www.lightreading.com/distributed-feedback-(dfb)-lasers/d/d-id/575160

<1% match (publications)
Vladimir Tejkal, Miloslav Filka, Jan Sporik, Pavel Reichert, Petr Munster. "The influence of binary modulations in passive optical network based on WDM", 2011 34th International Conference on Telecommunications and Signal Processing (TSP), 2011

<1% match (Internet from 11-Mar-2012)
http://www.pttimeeting.org

<1% match (Internet from 24-Mar-2016)
http://www.eudoxuspress.com

<1% match (publications)
Andreas Hornsteiner. "Fiber Optic Technology Trends in Data Transmission", Optik & Photonik, 2017

<1% match ()
Predehl, Katharina. "A 920 km optical fiber link for frequency metrology at the 19th decimal place", Ludwig-Maximilians-Universität München, 2012

<1% match (Internet from 03-Mar-2010)
http://etd.caltech.edu